PURIFICATION AND CHARACTERIZATION OF TWO EXTRACELLULAR PROTEASES WITH UNUSUAL PEPTIDE BOND SPECIFICITY FROM *XANTHOMONAS CAMPESTRIS* PV. *MALVACEARUM*

By

JING HUANG

Bachelor of Science

Shenyang Agricultural University

Shenyang, China

1982

Submitted to the Faculty of the
Graduate College of the
Oklahoma State University
in partial fulfillment of
the requirements for
the Degree of
MASTER OF SCIENCE
May, 1992

PURIFICATION AND CHARACTERIZATION OF TWO EXTRACELLULAR PROTEASES WITH UNUSUAL PEPTIDE BOND SPECIFICITY FROM *XANTHOMONAS CAMPESTRIS* PV. *MALVACEARUM*

Thesis Approved:

Robert K. Gholson
Thesis Advisor

Earl D Mitchell, Jr

Margaret L. Pierce

Thomas C. Collins
Dean of the Graduate College

ACKNOWLEDGMENTS

I would like to express my deepest appreciation to my major advisor Dr. Robert K. Gholson for his inspiring guidance, support and friendship during the course of this work. I would like to thank the other members of my graduate committee: Dr. Margaret L. Pierce and Dr. Earl D. Mitchell, Jr., for their suggestions, sympathy and assistance.

In addition, I would like to thank Dr. Andrew J. Mort for his advice and permission to use the equipment in his laboratory, Mr. Paul West for his help with the MS analysis of my peptides samples, to Dr. Earl D. Mitchell, Jr. and Ms. Janet Rogers for helping with my experiments, and to Dr. Jerry Merz for his help with computer analysis of data.

Moreover, I would also like to thank Dr. Margaret Essenberg, Carol R. Roberts, Gordon Davis, Edgar T. Miranda, Dr. Xiaoyang Qi, Dr.Feng Qiu and Robin Hurst for their suggestions, assistance and friendship .

Finally, I am indebted to my husband, my son, and my parents for their support, affection, patience and understanding during all these years. Special appreciation goes to my husband, Jinhua; It would not have been possible for me to finish this work without his constant encouragement and patient assistance.

TABLE OF CONTENTS

LIST OF TABLES

LIST OF FIGURES

Figure Page

LIST OF ABBREVIATIONS

AA	amino acid
AMPSO	3-[(1,1-Dimethyl-2-hydroxyethyl) amino] -2-hydroxypropanesulfonic acid
AUFS	absorbance units for full scale
BES	N, N bis [2-Hydroxyethyl] 2-aminoethane-sulfonic acid
CM-52	carboxymethyl cellulose pre-swollen 52 type
BCA	bicinchoninic acid
DEAE	diethylaminoethyl
ESI-MS	Electrospray Ionization-Mass Spectrometry
EPS	exopolysaccharide
EPPS	N-[2-Hydroxyethyl] piperazine-N'-3-propanesulfonic acid
HPLC	High-Performance Liquid Chromatography
HR	hypersensitive reaction
LSIMS	liquid secondary ion mass spectroscopy
MES	2[N-Morpholino] ethanesulfonic acid
MOPS	3-[N-morpholino] propanesulfonic acid
M.W.	molecular weight
NTG	N-methyl-N'-nitro-N-nitrosoguanidine
OD	optical density
P-1	protease-1 from *Xcm*
P-3	protease-3 from *Xcm*
PITC	phenylisothiocyanate

PMSF	phenylmethylsulfonylfluoride
PTC-AA	phenylthiocarbamyl Amino Acid
RPC	reverse phase chromatography
SDS-PAGE	sodium dodecyl sulfate polyacylamide gel
Xcm	*Xanthomonas campestris* pv. *malvacearum*

CHAPTER I

INTRODUCTION

Xanthomonas campestris pv. *malvacearum (Xcm)* is the causal agent of bacterial blight, a world-wide cotton disease. Even though the pathogen, the disease symptoms, the disease distribution and the host plant are well defined, the detailed biological mechanism for pathogen-host interaction in this disease is still poorly understood. However, some evidence is available which indicates a role for extracellular bacterial enzymes in pathogenicity. Venere *et al.* in 1986 reported the appearance of pectic enzymes (polygalacturonases and polymethylgalacturonases) preceding necrosis in leaves of susceptible cotton plants, as well as those resistant to cotton blight. At certain times after inoculation by infiltration of susceptible and resistant cotton cotyledons with *Xcm*, tissue extracts released reducing sugars when incubated with pectin, a major polysaccharide component present in cotton cell walls. This is due to action of pectic enzymes in the extract upon the substrate pectin, suggesting that pectic enzymes might be involved in the pathogen-host interaction (Verma, 1986). One of the strains tested by Verma and Singh in 1975 (*Xcm*-59) that had lost some of its virulence had, at the same time, also become weak in cellulase production, suggesting that cellulase is important for maintaining the virulence of the pathogen as well as for production of disease symptoms by this strain (Verma and Singh, 1975, as cited in Verma, 1986, p102).

Appreciable extracellular proteases are produced by almost all the pathogenic strains of *Xcm* (Verma, 1986). However, the role of extracellular protease in bacterial plant disease has been little investigated by genetic methods. Gholson *et al.* (1989) reported that protease-deficient mutants of *X. campestris* pv. *malvacearum* show reduced disease

symptoms and bacterial populations in the host plant. Some evidence from other *Xanthomonas* pathovars also supportes the involvement of extracellular protease in pathogen-host interaction. Xu and Gonzalez (1989) reported that an extracellular protease isolated from *Xanthomonas campestris* pv. *oryzae* might play an active role in leaf blight of rice. Tang, in 1989, demonstrated that the protease produced by *Xanthomonas campestris* pv. *campestris* is required for normal pathogenicity to plants (Tang, 1989, as cited in Liu *et al.*, 1990). Also, two extracellular proteases which have been purified from *Xcc,* the causal agent of black rot disease of cruciferous plants, were suggested to have a role in black rot pathogenesis by this organism (Dow *et al*., 1990).

To understand whether the proteases from *Xanthomonas campestris* pv. *malvacearum* play a role in cotton blight pathogenesis, the extracellular proteases from an Oklahoma field isolate of *Xcm* were investigated. The first part of this work describes the fractionation and purification of the enzymes from a culture supernatant of the bacterium. The second part of this work describes the characterization of properties of these enzymes which include optimal pH studies, inhibitor studies, and proteolytic specificity studies.

CHAPTER II

LITERATURE REVIEW

Xcm and Cotton Blight

Xanthomonas campestris pv. *malvacearum* (*Xcm*) is a gram-negative, strictly aerobic, motile, rod shaped, yellow-pigmented bacterium with a single polar flagellum. The species of *Xanthomonas campestris* contains 125 pathovars, including *malvacearum* , distinguished by their pathogenicity on host species. The yellow pigments, xanthomonadins of *Xanthomonas* spp. are a set of brominated aryl-polyene esters. Production of xanthomonadin is the primary factor distinguishing *Xanthomonas* spp. from the plant pathogenic *Pseudomonas* spp. which do not have this ability (Starr, 1981). *Xanthomonas* spp. also produce copious amounts of exopolysaccharide slime (EPS), also known as xanthan gum. The sugar composition of the EPS is uniform and independent of carbon sources. The majority constituent sugars are glucuronic acid, glucose and mannose. These three components sometimes accounted for 99% of the isolated EPS. The amount of EPS produced is influenced by culture conditions and the maximum is produced on mannose (one of the constituent sugars of EPS) where, incidentally, the amount was correlated with virulence (the most virulent race produced the greatest amount of EPS when grown on mannose while the least virulent race produced the least EPS. It was found that there was no such correlation between virulence and EPS production on glucose or starch, where only small amounts of EPS were produced. There was, however, some correlation when sucrose or galactose were the carbon sources (El-Banoby and Rudolph, 1979; El-Banoby *et al.*, 1981). Recently, Borker and Verma found that the most virulent race they tested produced the highest amount of EPS (1.761 mg/ml of total cultural filtrate) with

higher protein content (4%) as compared to a moderately virulent race (0.81 mg/ml), while an avirulent race produced only a minor amount (0.40-0.65 mg/ml) of EPS with less protein (1.5-2%) content (Borkar and Verma, 1990). This slime is also most likely the factor which leads to the predominant water-soaking observed in compatible interactions (El-Banoby and Rudolph, 1979; El-Banoby *et al.*, 1981). Under optimal conditions, lesions in the field have been noted to exude slime and are quite glossy in appearance (Brinkerhoff *et al.*, 1984). Auxotrophic mutants of *Xanthomonas campestris* pv. *vignaeradiatae* which produced less EPS were found to be less virulent than the wildtype bacteria (Thakur *et al.*, 1978).

Bacterial blight of cotton is generally considered as a parenchymatous disease, but it has now been shown that the vascular bundles can also be penetrated. Plants at all stages of development are affected, resulting in four phases of the disease, namely angular leaf spot (on the leaf), blackarm lesions (on stems and petioles), boll rot and gummosis (on bolls) and seedling blight (on seedlings). All the phases of the disease can be induced by the same isolate of the pathogen, *Xcm* (Verma, 1986).

One of the major resistant reactions of plants to bacterial infection is the hypersensitive reaction (HR). In the cotton-*Xcm* system HR is also observed as a rapid necrosis and collapse of the host tissue. During the susceptible reaction, disease symptoms are produced and high bacterial populations are reached within the susceptible host tissues. In an incompatible interaction, the HR was observed and the concentration of the pathogen in resistant host tissue did not reach more than 0.001 of the susceptible combination. This observation was based on an experiment in which cotton cotyledon tissues of the immune line Im-216 and the susceptible line Ac-44 were inoculated with *Xcm* and were incubated in a humid flask (Cason, 1977). The physiology of the interaction has been intensely studied. *Xcm* is known to induce the accumulation of phytoalexins in cotton cells adjacent to infection sites in incompatible interactions at levels sufficient to be bacteriostatic in culture (Essenberg *et al.*, 1986). Essenberg *et al.* noted that phytoalexins are bacteriostatic and bacteriocidal in some concentrations to growth of *Xcm* in culture and have greater toxicity to

Xcm in the presence of light than in the dark (Essenberg *et al.*, 1986; Sun, 1987; Sun *et al.*, 1988; Steidl, 1988; Essenberg *et al.*, 1990). Estimation of local concentrations of phytoalexins in fluorescent cells indicates that during incompatible interactions, there are concentrations exceeding those required for complete bacterial inhibition attained at all bacterial colonies on the day when bacterial multiplication stops. The phytoalexins are localized in the right place to be effective: in the leaky, dead or dying mesophyll cells closest to the intercellular bacterial colonies. Essenberg and Pierce (1992) concluded phytoalexin accumulation is a part of the resistant response of cotton foliar tissue to bacterial pathogens. Although the production of phytoalexins may be probably the biggest component of resistance, there is no direct evidence linking induction of phytoalexin production with bacterial avirulence gene expression.

Physical events associated with the interaction are also well defined. The interaction with both susceptible and immune cotton leaves can be initiated by a single cell of *Xcm* which grows into a colony. Bacterial growth can have a logarithmic phase in susceptible and immune leaves, producing expanding water-soaked areas in susceptible leaves. However in immune leaves bacterial growth stopped at lower population densities and small clusters of dark brown host cells developed. The immune leaf responds locally to each bacterial colony (Cason *et al.*, 1977, 1978; Essenberg *et al.*, 1979a, 1979b; Al-Mousawi *et al.*, 1982, 1983; Morgham *et al.*, 1988).

The role of enzymes of *Xcm* in pathogenicity is not clear. Generally speaking, when a pathogen infects a host it has two alternatives (pathways). It will either produce the pathogenicity factor or it will repress it, which may even be a host-directed response. Alternatively, the polysaccharides of the pathogen can specifically induce (as a substrate) the formation of a protein (enzymes) in the host and the polysaccharide must be broken down to release the pathogenic factor. Very limited information about virulence factors within *Xanthomonas* spp. is available at present. Verma and Singh reported that leaf discs of Acala 44 (susceptible) were macerated whereas 101-102B (resistant) discs were not when

they were treated with crude extracellular pectic enzymes produced by *Xcm*. This was also confirmed by a higher Klett reading of the supernatant of the reaction mixture, which had turned very green in susceptible tissues due to maceration and release of chloroplasts. It was concluded that although pectic enzymes were produced in low quantity by *Xcm*, maceration of tissues did play a role in pathogenesis (Verma and Singh, 1975). Cellulases were present in the crude extracellular enzyme preparations of two isolates of *Xcm* cultured on NB or NB+ pectin. One of the strains (*Xcm*-59) that had lost some of its virulence had, at the same time, also become weak in cellulase production. Verma and Singh considered that cellulases play an important role in the disease reaction (Verma and Singh, 1975). Gholson and Essenberg (1987) reported that a N-methyl-N'-nitro-N-nitrosoguanidine (NTG)-induced mutant (PM1) of *Xcm* race 3631 was deficient in protease in media containing proteins as sole nitrogen source and had 20-25% of the protease activity of race 3631 under optimal inducing conditions. Further NTG mutagenesis of PM1 produced a mutant (PM2) which does not grow on proteins as N source and produces no detectable protease, either in vitro or in planta. When leaves of susceptible cotton (Acala 44) were inoculated with PM2, water-soaked lesions developed more slowly and were smaller than lesions arising from race 3631 or PM1, indicating that PM2 has decreased pathogenicity. Daniels *et al.* have identified genes for pectinolytic and proteolytic enzymes associated with the pathogenesis of *Xcc* on crucifers, and two proteases (PRT1 and PRT2) were later isolated from culture supernatants of wild-type *Xcc* (Daniels et al., 1984). A protease-deficient mutant which lacked both PRT1 and PRT2 showed reduced symptoms when bacteria were introduced into mature turnip leaves (Dow *et al.*, 1990). Xu and Gonzalez (1989) reported that protease-deficient mutants of *Xco*, the causal organism of bacterial leaf blight of rice, were reduced in pathogenicity and populations *in planta* were 1 to 10% of those observed for the parental strain, indicating that proteases may be involved in pathogenesis.

Proteases and Their Specificities

Of the extracellular proteins investigated, the proteolytic enzymes have received considerable attention, and study of their properties has significantly contributed to the elucidation of the relationship between the structure and function of enzymes. Proteases are classified into four groups according to their catalytic mechanisms, that is, serine proteases, cysteine proteases, aspartic proteases and metallo-proteases (Barrett, 1980). A view of the catalytic mechanism of the serine proteases would be that initially the hydroxyl group of the active site serine residue attacks the carbonyl carbon atom of the substrate, with general base catalysis by histidine. For cysteine proteases, the thiolate- imidazolium ion pair is the reactive nucleophile. An acyl enzyme is formed with the thiol of cysteine and hydrolyzed much like the serine proteases. The catalytic mechanism of aspartic proteases is consistent with a general acid- general base catalysis. The essential catalytic groups are carboxyl groups of aspartic acid. In the metallo-proteases the hydrolysis of peptide bonds can be catalized by metal ions through charge stabilization, water ionization and charge shielding.

The metallo-proteases are widespread in bacteria, streptomycetes and fungi, as well as in higher organisms. They differ widely in molecular weight, but very few amino acid sequence data are available for them. It seems probable that zinc is the catalytically active metal in the natural forms of all of the metallo-proteases. The molecules contain zinc and the addition of Zn^{2+}in the assay medium usually does not increase activity but may decrease it. The metallo-proteases typically show maximal activity at about pH 7.0 and prefer cleaving peptide bonds of residues having non-polar side chains (Barrett and Salvesen, 1986).

Traditionally the proteases have been regarded as degradative enzymes which are capable of cleaving proteins into small peptides and amino acids and whose role it is to digest nutrient protein or to participate in the turnover of cellular protein. Indeed, this is true of the best characterized of the proteases, such as trypsin, chymotrypsin and pepsin. More

recently, however, it has also been demonstrated that limited proteolysis has a key role in a wide range of cellular processes. The ability of proteolytic enzymes to carry out selective modification of proteins by limited cleavage, as in the activation of hormones, for example, means that some proteinases have a regulatory function. This has added considerable interest to an already important group of enzymes. As a result of the recognition of more specific proteolytic processes and the use of more selective substrates, an increasing number of proteinases are being detected in all types of organisms (North, 1982).

Many eucaryotic microorganisms are pathogenic, causing diseases in plants as well as in animals. For the interaction between host and pathogen, protease may be needed by the latter to penetrate the host tissue or to utilize host protein for nutrition. There have been many demonstrations of proteolytic activity in cultures of fungi pathogenic to plants and also in infected plant material. However, few have provided direct evidence for a definite role for proteases in infection, but, a correlation between pathogenicity and proteinase activity has been reported. Ries and Albersheim considered the possibility that the proteases from *Colletotrichum lindemuthianum* might play a role in degrading the hydroxyproline-rich structural proteins of the host plant cell walls, since protease activity was secreted shortly after endopolygalacturonase activity (Ries and Albersheim, 1973). Roby *et al.*, in 1987 did experiments on the elicitation of proteinase inhibitors in melon leaves by *Colletotrichum lagenarium* infections or by treatment with cell wall preparations obtained from this fungus. The proteinase inhibitor was active against a trypsin-like protease produced by the pathogen during host infection or when grown on a plant cell wall containing liquid medium. This suggests a role for that protease in the disease process. Strong evidence for the requirement of extracellular protease in the pathogenic interaction of *Pyrenopeziza brassicae*, the causal agent of light leaf spot of brassicas, with oilseed rape was provided by Ball *et al.* (1991). Several mutants of *P. brassicae* deficient in the production of extracellular enzymes were isolated. The protease mutants were either non-pathogenic (NH10/247, NH10/540) or weakly pathogenic (JH26/571), suggesting that

extracellular protease production is a pathogenicity determinant. They considered that the extracellular protease may be involved in degradation of plant cell wall proteins or selective degradation of membrane proteins to perturb membrane transport functions as a means of providing nutrients to the growing mycelium.

Samsinakova *et al.* (1977) have found that the amount of protease and chitinase activity of both *Beauveria bassiana* and *Paecilomyces farinosus* correlated with their pathogenicity on the Colorado beetle. In addition, the idea that tissue lesions associated with invasive amoebiosis caused by *Erwinia histolytica* might be caused by proteases has been suggested by many workers. Lushbangh *et al* . (1981) have provided evidence in support of a direct relationship between a cytotoxin from *E. histolytica,* whose concentration correlates with strain virulence and protease activity, since cytotoxin activity can be inhibited by α-1 antiprotease.

Recently, Kyostio *et al.*, (1991) characterized the *prt* 1 gene for extracellular metalloprotease from *Erwinia carotovora* subsp. *carotovora* EC 14 but , so far, they do not know the significance of *prt* 1 in soft rot. However, the detection of elevated levels of *prt* 1 mRNA from *in planta* grown *Erwinia. carotovora* subsp. *carotovora* indicates that this protease is produced during potato maceration. Hinode *et al.* (1991) purified three types of proteases (Pase-A, Pase-B and Pase-C) from culture supernatants of *Porphyromonas gingivalis.* All three proteases are differently concerned with periodontopathogenesis not only in degrading periodontal tissues but also in decreasing host defense capacity by degrading plasma proteinase inhibitors which have a role in host defense against tissue-invading bacteria. Bashan *et al.* in 1986 reported that there was a possible role for proteases and deaminases in the development of the symptoms of bacterial speck disease in tomato caused by *Pseudomonas syringae* pv. *tomato. P. syringae* pv. *tomato* produces constitutive proteases during the logarithmic phase of growth in culture. Proteolytic activity was higher (per bacterium) in the diseased tissue of susceptible plants than in resistant plants, reaching maximum levels during the later stages of infection. A

correlation between disease severity and proteolytic activity in infected tissue was demonstrated, with activity being greatest around developing necrotic zones. The activity also varied with the age of the leaf at the time of infection. The addition of asparagine and glutamine to infected suceptible plants, increased disease severity and ammonia production. These results suggest that after the establishment of a massive *P. syringae* pv. *tomato* population in plant tissue (after recognition, penetration, multiplication, primary cell collapse and possible liberation of proteins and amino acids), the pathological interaction produces proteolytic enzymes which degrade plant proteins to amino acids. These amino acids are then deaminated, particularly asparagine and glutamine by asparginase and glutaminase, resulting in the production of large quantities of ammonia. This leads to an increase in plant tissue pH at later stages of disease development. At pH 8.0 and above, the ammonia is liberated as gaseous ammonia, which diffuses through the intercellular spaces and causes leakage of electrolytes. This chain of events was suggested to result in cell death and in the initiation of the necrotic lesion.

Of the many proteases which have been characterized, only a very few are so specific that they cleave peptide bonds adjacent to only one amino acid. A protease purified from the culture filtrate of *Streptococcus aureus*, strain V8, specifically cleaves peptide bonds on the C-terminal side of both aspartic and glutamic acid residues in phosphate buffer. However, in ammonium bicarbonate or ammonium acetate buffer, it only cleaves on the C-terminal side of glutamic acid (Drapeau *et al.*, 1972). Walton *et al.* (1972) have isolated a protease from the fruiting body of the basidiomycete *Armillaria mellea.* This enzyme has been shown to be an endopeptidase cleaving proteins such as fibrinogen and casein N-terminal to lysine residues. Further characterization of this enzyme indicated that this specific hydrolysis is prevented by an aspartic acid residue C-terminal to lysine and impeded in some cases by glutamic acid on either side of the lysine residue (Doonan *et al.*, 1974; Walton *et al.*, 1972). Interestingly, another protease purified from *Lysobacter enzymogenes* cleaves only C-terminal to lysine residues (Keesey, 1987) and a protease from

mouse submaxillary gland cleaves only C-terminal to arginine (Levy *et al.*, 1970). In 1979, Noreau and Drapeau reported that a metallo-protease secreted by the wild type of *Pseudomonas fragi* cleaves N-terminally to several amino acids having small hydrophilic residues (Noreau and Drapeau, 1979). However, a mutant of this organism, selected for its ability to grow on elastin following NTG mutagenesis, secreted five proteases with altered specificities. One of these proteases cleaves specifically the peptide bonds on the N-terminal side of either aspartic acid or cysteic acid residues (Drapeau, 1980). However, a later report indicates that the *P. fragi* protease also cleaves N-terminal to some glutamic acid residues in some proteins in addition to the expected cleavage sites at aspartyl residues (Ingrosso *et al.*, 1989). An aminopeptidase A (EC 3, 4, 11, 7) was purified from *Lactococcus lactis* subsp. *lactis* NCDO712. Of the 18 aminoacyl-alanine dipeptides tested, the enzyme hydrolyzed Asp-Ala, Glu-Ala,and Ser-Ala (Niven, 1991). Of the three proteases (Pase-A, Pase-B and Pase-C from *Porphyromonas gingivalis*) studied by Hinode *et al.* (1991), Pase-A, which is a serine protease, cleaved the peptide bonds Glu-Ala and Ala-Leu of insulin.

Proteases have proved to be valuable reagents in laboratory, clinical, and industrial processes. They also play an essential role in a number of food processes involving microorganisms. Purified proteases with high peptide bond specificities are very useful for protein sequence analysis (Shipolini *et al.*, 1974; Barry *et al.*, 1981; Doonan and Fahmy, 1975) and peptide synthesis (Royer *et al.*, 1980; Widmer and Johansen, 1979).

CHAPTER III

MATERIALS AND METHODS

Materials

Skim-milk and nutrient broth were purchased from Difco Laboratories. Bicinchoninic acid (BCA) protein assay reagent, amino acid standards, and trifluoroacetic acid (TFA) were all from Pierce Chemical Co. Carboxymethyl cellulose CM-52 and diethylaminoethyl cellulose DEAE were from Whatman Chemical Co. Azocasein, 3-[N-morpholino] propanesulfonic acid (MOPS), octyl-sepharose CL-4B, oxidized insulin A chain, oxidized insulin B chain, glucagon, phenylmethylsulfonylfluoride (PMSF), 1,10-phenanthroline, trypsin, and thermolysin were purchased from Sigma Chemical Co. Phosphoramidon and 3,4-dichloroisocoumarin were purchased from Calbiochem. All other chemicals were of reagent grade.

Bacteria and Culture Conditions

Bacteria

The *Xcm* strain 3631 used in these studies is a spontaneous streptomycin-resistant mutant of the highly aggressive field isolate from Altus, Oklahoma, that was previously described by Essenberg *et al.* (1982). Bacteria were amplified in 150 ml nutrient broth in a 1000-ml flask with a side arm, growing at 30° C for about 24 h, until an optical density of 0.25 (OD_{600}) was reached. (The absorbance was measured with a Coleman Junior Spectrophotometer). After harvesting the bacteria by centrifugation, the bacteria were

resuspended in 15 ml of 14% glycerol and 86% nutrient broth and dispensed in 1.5 ml microcentrifuge tubes (1 ml per tube), followed by freezing with dry ice/ acetone. The bacterial suspension was then stored at -70° C for future use.

Culture Conditions

To further amplify the bacteria, 50 ml of nutrient broth in a 250-ml flask with a side arm was inoculated with a scoop of the frozen bacteria under a flame. The flask was shaken at 180 rpm at 30° C for about 24 h until an optical density of about 0.1 (OD_{600}) was reached. In a sterile hood, the bacterial suspension was centrifuged in four 12 ml centrifuge tubes at full speed in an I.C.E. clinical centrifuge for 10 min. After discarding the supernatant, the bacteria were resuspended in saturated $CaCO_3$ (1 ml /tube), and transferred into 3 two-liter Erlenmeyer flasks with 750 ml of defined MOPS buffered medium developed by Neidhardt *et al.* (1974) and modified by McNally *et al.* (1984), The amino acids added to Neidhardt's MOPS medium and their concentrations were: L-alanine, 0.47 mM; L-arginine-HCl, 0.60 mM; L-asparagine, 0.32 mM; L-histidine-HCl, 0.10 mM; L-isoleucine, 0.30 mM; L-threonine, 0.30 mM; and L-phenylalanine, 0.30 mM. Glycerol at 1.0% (v/v) was used as the carbon source. For routine protease production, the ammonium chloride in this medium was replaced with 0.1% skim-milk plus 0.1% L-glutamic acid as the nitrogen source. This was tested by Gholson and Roberts (Figures 1 and 2).

Figure 1. Time course of growth of *X. campestris* pv. *malvacearum* strain 3631 on various nitrogen sources. Cultures (25 ml) were grown in 125-ml Erlenmeyer side-arm flasks at 30° C with shaking at 180 rpm in MOPS-buffered minimal medium with various nitrogen sources. Nitrogen sources: – ■ –, none (except the 7 amino acids with total concentration 4.4 mM present in all cultures); – o –, 9.5 mM NH_4Cl; – Δ –, 0.1% L-aspartic acid; – ● –, 0.1% L-glutamic acid; – ▫ –, 0.1% skim-milk; – + –, 0.1% skim-milk plus 0.1% glutamic acid; – ▲ –, 0.1% tryptone. Growth was monitored by measuring OD_{600} of the flask contents tipped into the side arm (unpublished data of Gholson and Roberts).

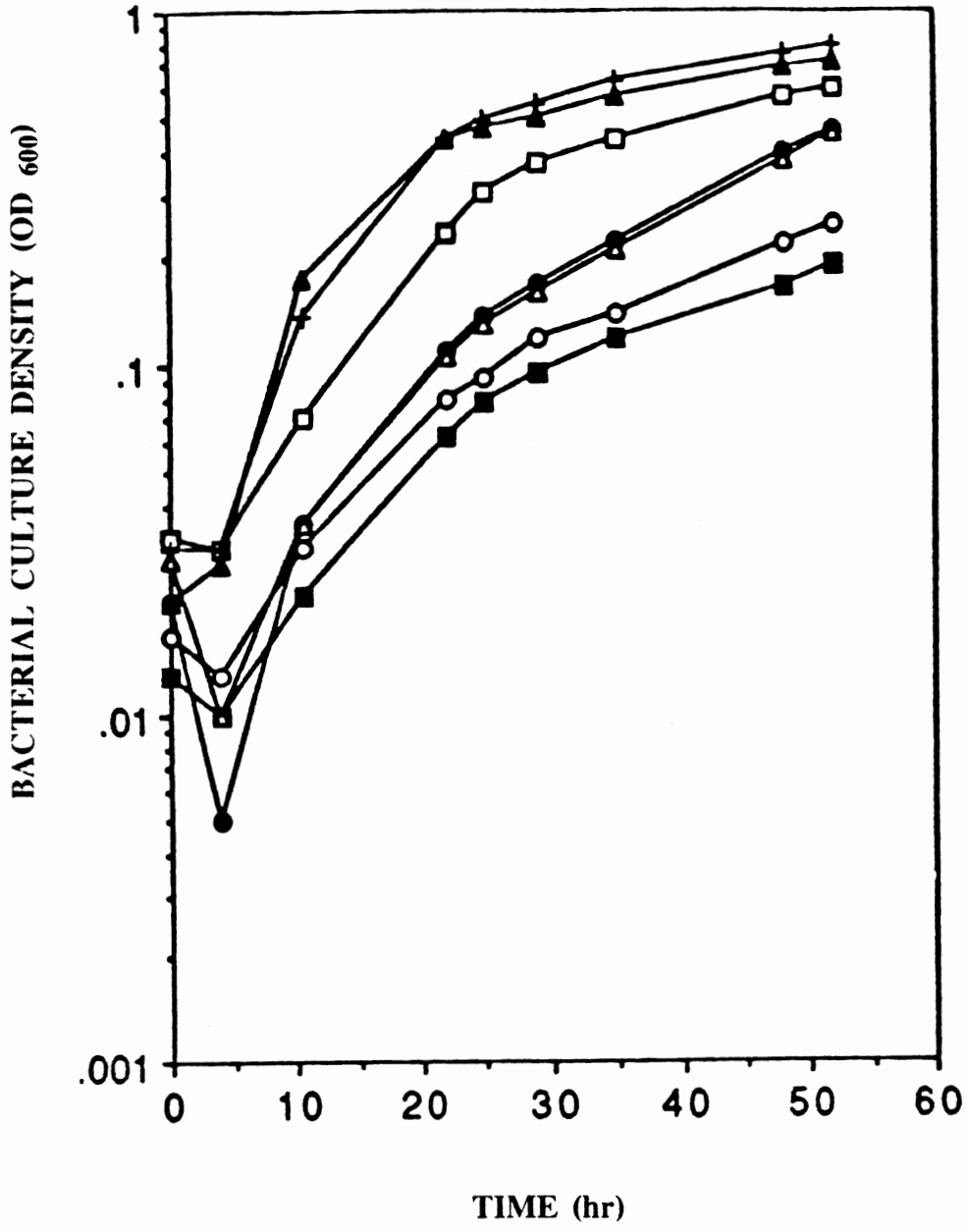
BACTERIAL CULTURE DENSITY (OD 600)
1
.1
.01
.001
0
10
20
30
40
50
60
TIME (hr)

Figure 2. Protease production as a function of growth on various nitrogen sources. When OD_{600} reached *ca.* 0.2 (Figure 1), 1.0-ml aliquots were removed at every OD_{600} reading for protease assay using azocasein as substrate. Protease activity (A_{370}) was plotted as a function of bacterial growth (OD_{600}) on each nitrogen source. Symbols indicate the same nitrogen sources as in Figure 1 (Unpublished data of Gholson and Roberts).

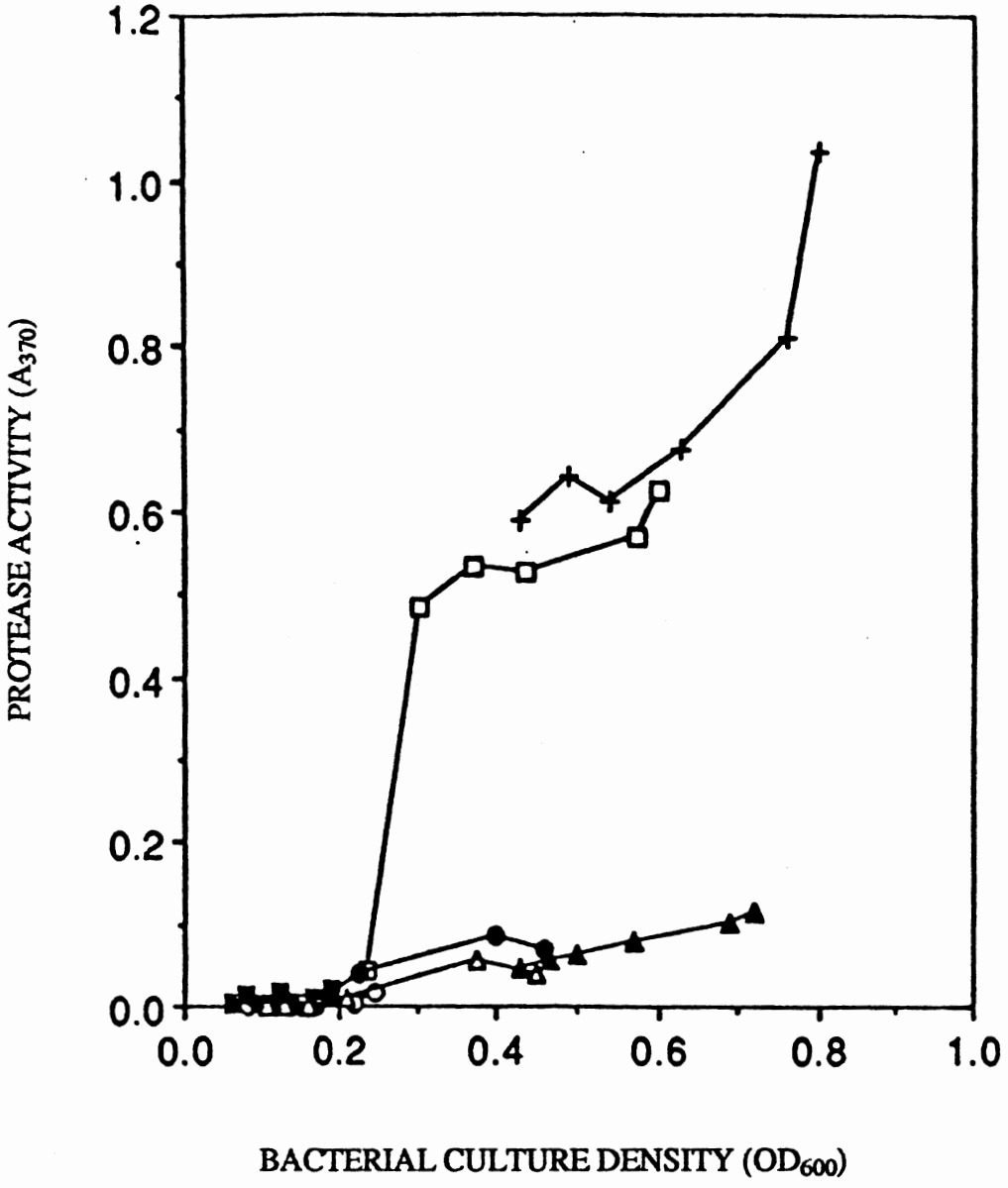
1.2
1.0
0.8
0.6
0.4
0.2
0.0
0.0
0.2
0.4
0.6
0.8
1.0
PROTEASE ACTIVITY (A_{370})
BACTERIAL CULTURE DENSITY (OD_{600})

Procedure of Protease Purification

Carboxymethyl Cellulose CM-52 Cation Exchange Chromatography

Three flask cultures totaling 2250 ml were grown with shaking at 180 rpm at 30° C for 40 h to an apparent optical density (OD_{600}) of 0.5 ~ 0.6. Bacterial cells were removed from the cultures by centrifuging with a GSA rotor at 10,000 rpm for 25 min at 4° C. The supernatant (2250 ml) of the culture was then mixed with 130 ml of Whatman Carboxymethyl Cellulose CM-52 (pre-swollen ion exchange cellulose) and stirred at 4° C overnight. This resulted in the disappearance of detectable protease activity from the supernatant. The remaining steps were also carried out at 4° C. The CM-52 cellulose column material with adsorbed protease was allowed to settle for 1 h, and the supernatant was decanted. The CM-52 cellulose column material plus protease was slurried in 0.01 M Tris-HCl, pH 7.5, and poured into a 50 X 2.5 cm (Econo-Column purchased from Bio-Rad) chromatography column. The column was washed (0.3~0.4 ml/min) with the same buffer until the absorbance of the effluent at 280 nm was the same as the buffer. Protease activity was then eluted from the column with a linear gradient of 0.0 M NaCl in 0.01 M Tris-HCl buffer, pH 7.5, to 1.0 M NaCl in 0.01 M Tris-HCl, pH 7.5, by using a gradient mixer that accommodates 150 ml on each side. Five milliliter fractions (99 drops) were collected and assayed for protease activity and protein concentration. The protease activity was eluted between 80 to 150 ml.

Diethylaminoethyl Cellulose Anion Exchange Chromatography

The active fractions with A_{370}>0.2 from the CM-52 column were combined, and adjusted to pH 9, and then were loaded on a Diethylaminoethyl (DEAE) Cellulose column (17 ml bed volume). This was done at 4° C with flow rate about 0.5 ml/ min. All flow-through fractions which contained protease activity were saved and adjusted back to pH 7.5. Since DEAE cellulose is marketed in powder form, all stages of pre-treatment were carried

out as described by Whatman Biosystems Inc. in order to obtain the best possible performance. The weighed ion exchange resin was stirred into 15 vols. (w/v) of 0.5 M HCl for 30 min followed by filtering the supernatant and washing with distilled water until the filtrate was at the intermediate pH 4. The slurry was then stirred into 15 vols. of 0.5 M NaOH for 30 min followed by washing with distilled water until the filtrate was near neutral. The pre-treated ion exchanger was equilibrated with 0.01 M Tris-HCl buffer pH 9 and was ready to be used.

Concentration of Protease Solutions

Ultrafiltration of protease fractions from the DEAE column was done using a stirred Ultrafiltration Cell equipped with a Diaflo YM 10 membrane (Amicon, Lexington, MA.). The protease solutions were concentrated down to 20 ml.

Octyl-Sepharose CL-4B Reverse-Phase Chromatography

The concentrated protease solution was made 4.0 M in NaCl with solid salt, and applied directly to a 3.5 ml Octyl-Sepharose CL-4B Column which had been equilibrated with 4.0 M NaCl in 0.01 M Tris-HCl, pH 7.5. The proteases were adsorbed to the Octyl-Sepharose under these conditions and were eluted using a step gradient of decreasing NaCl concentrations (4.0 M, 3.0 M, 2.0 M, 1.0 M, 0.0 M) in 0.01 M Tris-HCl, pH 7.5, and two 5 ml fractions were collected at each salt concentration and assayed for protein concentration and protease activity. Active fractions were individually dialyzed against distilled water, lyophilized, and dissolved in H_2O for sodium dodecyl sulfate polyacrylamide gel electrophoresis (SDS-PAGE) and other studies (Figure 3).

Figure 3. Scheme for protease purification showing that proteases were isolated and purified from culture supernatants of *Xanthomonas campestris* pv. *malvacearum* by the combined procedures of ion-exchange chromatography, ultrafiltration and reverse phase chromatography.

PROTEASE PURIFICATION SCHEME

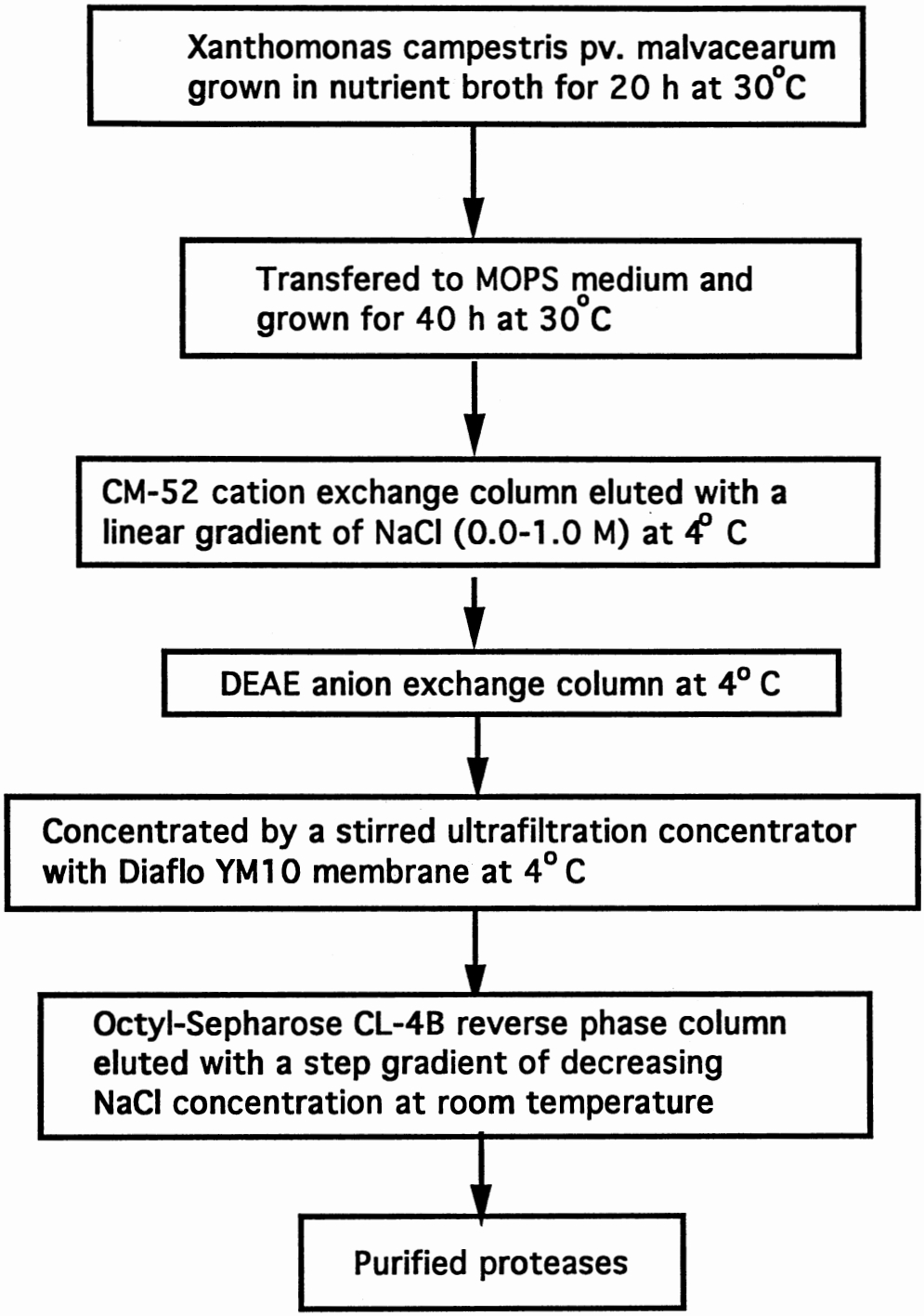

Chemical Analysis

Enzyme Assays

Protease activity in crude supernatants and purified fractions was assayed spectrophotometrically using azocasein at A_{370} as described by Jenson *et al.* (1979). The coupling of a protein with a diazotized aryl amine will produce a chromophoric derivative. Such an azoprotein may be precipitated from solution by trichloroacetic acid to yield a colorless filtrate. If the azoprotein solution is subjected to proteolytic digestion, colored reaction products are formed which are soluble in trichloroacetic acid solution. The intensity of color in the trichloroacetic acid filtrate of the digested substrate is a function of the proteolytic activity of the enzyme solution (Figure 4). The reaction mixture contained 0.25 ml of azocasein reagent (A fresh batch of 1% azocasein in distilled water was made each time it was used), 0.25 ml of 0.01 M Tris-HCl buffer (pH 7.5), and 0.5 ml of enzyme solution. The reaction mixture was stopped after 15 min of incubation at 30° C by the addition of 1 ml of 10% cold trichloroacetic acid. After standing for 30 min at room temperature, the absorbance at 370 nm of the filtrate (by Whatman #7 filter paper) was measured. One unit of activity was defined as the amount of enzyme needed to produce an increase in absorbance at 370 nm of 1.0 in 1 min under standard assay conditions. Figure 4 shows the proportionality of absorbance to protease concentration.

Determination of protein concentration

Protein concentration was determined as described by Smith *et al.* (1985). Bicinchoninic acid (BCA) working reagent was prepared by mixing 50 parts Reagent A (BCA) with 1 part Reagent B (4% $CuSO_4$). Both Reagent A and Reagent B were purchased from the Pierce Chemical Company, Rockford, IL.

First, a set of protein standards was prepared by diluting the BSA stock solution to make a series of 25, 50, 100, 150, 200, and 250 microgram per milliliter, respectively,

(Figure 5). The reaction mixture containing 0.1 ml of each standard or unknown protein sample was mixed with 2.0 ml of BSA working reagent and incubated at 60° C for 30 min. After incubation, the reaction mixtures were cooled to room temperature, and the absorbance was measured at 562 nm against a blank made of water. Finally, the protein concentrations were determined by comparing to the standard curve (Figure 5).

Figure 4. Demonstration of the proportionality of absorbance to protease concentration in the azocasein assay for protease activity by varying the amount of protease (0, 50, 100, 150, 200, 250, 500 µl of protease from CM-52 crude proteases) in the reaction mixture while all other factors were kept constant.

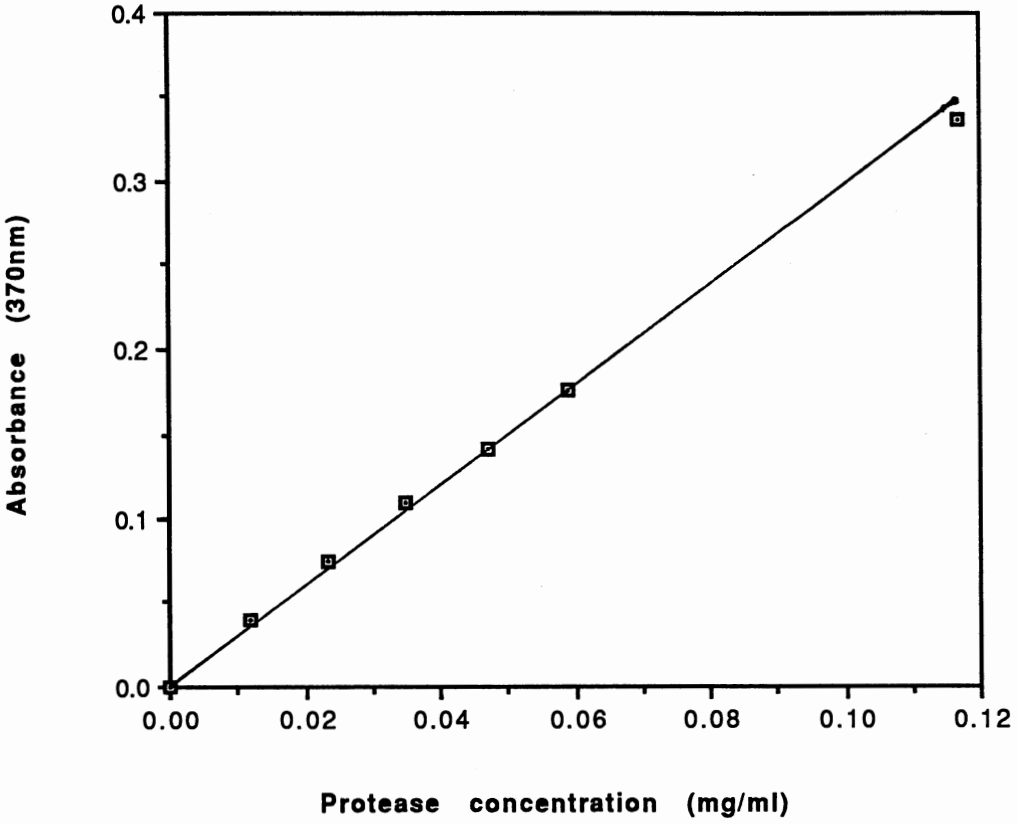
0.4
0.3
0.2
0.1
0.0
Absorbance (370nm)
0.00
0.02
0.04
0.06
0.08
0.10
0.12
Protease concentration (mg/ml)

Figure 5. Standard curve for protein concentration determination. Protein standard concentrations were 0.0, 0.025, 0.05, 0.10, 0.15, 0.20, 0.25 mg BSA/ml. Standards (0.1 ml) were incubated for 30 min. at 60° C with BCA reagent (2.0 ml).

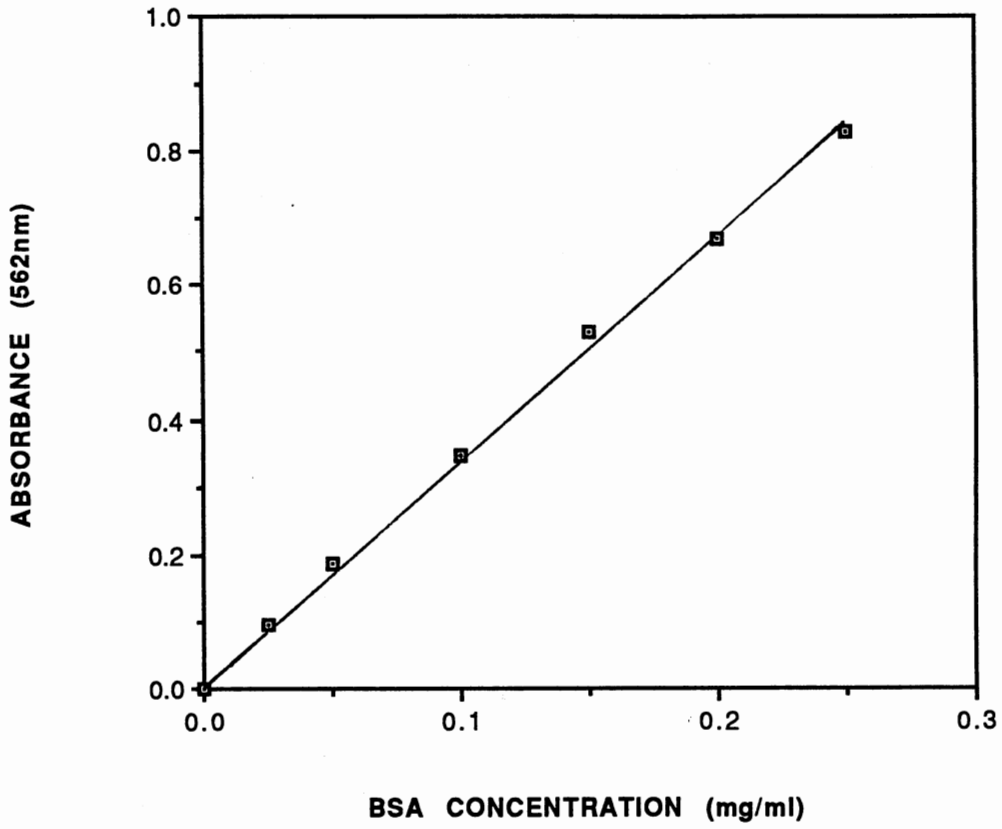
1.0
0.8
0.6
0.4
0.2
0.0
ABSORBANCE (562nm)
0.0
0.1
0.2
0.3
BSA CONCENTRATION (mg/ml)

Analytical Methods

Gel Electrophoresis

SDS-PAGE of the enzyme fractions was carried out as described by Weber *et al.*,(1976) using 10% polyacrylamide gels (1.5 mm thick) in a mini protein II Dual Slab Cell System (Bio-Rad Laboratories, Richmond, CA.). Polyacrylamide concentrations in the separating and stacking gels were 10 and 4% respectively. The samples were run for 1 h at a voltage equal to 100 volts while maintaining a constant current. The gels were stained with 0.1% coumassie blue in 25% isopropanol / 10% acetic acid. Low molecular weight standards (Bio-Rad Laboratories) were run and are as following: rabbit muscle phosphorylase b is 97,400 Da, bovine serum albumin (BSA) is 66,200 Da, hen egg white ovalbumin is 45,000 Da, bovine carbonic anhydrase is 31,000 Da, soybean trypsin inhibitor is 21,500 Da, hen egg white lysozyme is 14,400 Da. The gels were destained with 20% methanol and 7% acetic acid for 24 h until the background was clear and the bands were bright blue.

Reversed Phase Chromatography (RPC)

The peptides produced by incubation of protease from *Xcm* with substrates (insulin A chain and B chain, glucagon, thymopoietin II fragment 32-36) were separated by HPLC (Beckman 110B Solvent Delivery Module) equipped with a Bakerbond wide-pore (30 nm) C-18 (5μm) reversed phase column (4.6 X 250 mm from J.T. Baker, Inc.). The following solvent system was used. Solvent A: 0.1% trifluoroacetic acid (TFA) in distilled water, solvent B: 0.09% TFA in acetonitrile/water 62.5 : 37.5 (v/v). Both solvents were degassed with sonication (Bransonic 220, Branson Cleaning Equipment Company) and water aspiration. The experiments were carried out with a Beckman 421A Controller at a flow rate of 1.0 ml / min. The peptides were eluted with a linear gradient of increasing acetonitrile concentration. Solvent B was increased linearly from 0 to 100% (v/v) over 55 min, and was

followed by elution at 100% solvent B for 10 min. Peptide-containing fractions were collected manually into Eppendorf tubes on a Gilson Model 203 collector, based on the UV absorption at 214 nm and sensitivity 0.2 AUFS with a Beckman 163 variable wavelength detector (Aebersold *et al.*, 1987).

Liquid Secondary Ion Mass Spectrometry (LSIMS)

Molecular weights of the peptide fragments generated by protease cleaving insulin A chain, insulin B chain, and glucagon, were identified by LSIMS. The peptide samples were dried using a Speed Vac Concentrator (from Savant Instrument Co., Farmingdale, NY). The dried samples were then dissolved in 2 to 5 µl of water and then 1 µl of the solution was mixed with 1 µl of thioglycerol on a stainless steel target before injection. Spectra were obtained on a ZAB 2SE mass spectrometer (from VG, Manchester, UK) using cesium ions at 35 KV for the ionization and were collected in the positive ion mode. Both $[M+H^{+}]$ and $[M+Na^{+}]$ ions were observed in most of the cases. Dr. Jinhua An from C.C.R.C., The University of Georgia and Mr. Paul West from the Chemistry Department of O.S.U. ran the peptide samples. The spectra were analyzed using a computer program for peptide M.W. calculation called MacProMass developed at the Beckman Research Institute of the City of Hope and written by Sunil Vemuri with Dr. Terry D. Lee. The program calculates the peptide M.W. generated from all the combinations of amino acids resulting from amino acid sequences of the substrate digested by the protease.

Electrospray Ionization Mass Spectrometry (ESIMS)

Molecular weights of peptide fragments generated by protease cleaving glucagon and Thymopoietin II Fragment 32-36 were identified by Electrospray Ionization Mass Spectrometry. Mass spectra were obtained on a PE-Sciex (Thornhill Canada) API III. ESIMS is interfaced to a Macintosh II spectro with Sciex software. Ion spray voltage was 5000 V. The peptide samples were dried using a speed Vac Concentrator, then dissolved in

150 µl buffer (50% CH_3CN, 0.1% formic acid and 2 mM ammonium formate). Ten µl was introduced into the mass spectrometer at 2 ml/min using a Harvard 22 syringe infusion pump. The mass range was scanned from 100-1200 amu (5 millisec. dwelltime, 10 scans were collected and averaged). $[M+H^+]$, $[M+Na^+]$ and $[M+NH_4^+]$ ions were observed in most of the cases. Dr. Jinhua An from C.C.R.C., The University of Georgia ran the peptide samples. The spectra were analyzed using the same program as for LSIMS.

CHAPTER IV

RESULTS AND DISCUSSION

Enzyme Purification

Proteases from the bacterium *Xcm* were purified as described in "protease purification scheme" in Chapter III. The whole process of purification took about eight days. Proteases are very stable enzymes: crude protease with absorbance (370nm) 0.405 which was stored at 4° C or frozen for 15 days still had activity with absorbance (370nm) 0.369. Purified, lyophilized protease can be kept in the freezer for a year, even though the proteases had lost some activity due to dialysis (loosing metal ions) and lyophilization.

The production of extracellular polysaccharide slime by *Xcm* complicated isolation of protease from culture supernatant and effectively prevented column chromatography of crude culture supernatants. Fortunately, the proteases were positively charged and could be efficiently adsorbed onto CM-52 cellulose from the supernatant by a batch process (see Materials and Methods). Supernatant was tested for protease activity and very little activity was present, but the majority of contaminating proteins apparently were in this supernatant (Protein concentration in the supernatant dropped slightly from 0.476 to 0.382 mg/ml. But protease activity dropped dramatically from 0.556 to 0.060 units/ml. Activity units are ΔA_{370}/15 min) indicating this step was very successful. The protease was then eluted from the CM-52 by a salt gradient. From the elution profile (Figure 6), it was noted that the majority of protease activity was eluted between tubes 17-30 and did not continue to co-elute with proteins that were eluted by a much higher concentration of salt. The protein and protease activity were eluted in roughly a single peak, centered on fraction 20 (Figure 6). The fractions (17-30) containing proteases were combined for further purification.

From the earlier work, it was found that, after CM-52 column chromatography, going directly to Octyl-sepharose CL-4B column chromatography was not efficient enough to get rid of contaminants and to purify protease-3 (without DEAE step, some contaminating protein was still mixed with protease-3 on the next step of the purification). Therefore the combined fractions from CM-52 cation exchange chromatography were first applied on a DEAE anion exchange column as the pH was changed from 7.5 to 9. Under these conditions, some contaminating protein with lower positive charge at pH 7.5 became negatively charged on surface at pH 9 and therefore bound to the DEAE column. In contrast, the proteases just went through the column. By this step, a mixture of three proteases (presumed) was obtained. From the SDS-PAGE result in Figure 7, it was noted that the eluate from DEAE column consisted of three proteins with M.W. of approximately 29,000 Da; 38,000 Da and 43,000 Da, respectively compared to the standard molecular weight markers. These three proteins were temporarily named as protease-1, protease-2 and protease-3 (Figure 7).

After concentration, with a Diaflo YM 10 membrane concentrator, the proteases were further purified individually by applying the mixture to a Octyl-sepharose CL-4B reverse phase column. The proteases were eluted from the column using a step gradient of decreasing NaCl concentrations in 0.01 M Tris-HCl buffer pH 7.5. Some purification of the proteases was obtained. Figure 8 coupled with Figure 9 shows that protease-1 was eluted by 3.0 M NaCl in Tris-HCl buffer, and Figure 8 coupled with Figure 10 shows that protease-3 was eluted by 0.0 M NaCl in Tris-HCl buffer. Protease-2 was in mixture with small amounts of protease-3 and was eluted by 2 M NaCl and 1M NaCl in Tris-HCl buffer (gel not shown).

The proteases yielded by these procedures as summarized in Table 1, appeared to be homogeneous on SDS-PAGE. Figure 9 shows the SDS-PAGE pattern of the protease-1, and Figure 10 shows the SDS-PAGE pattern of the protease-3 present at this stage of purification. From the enzyme purification table (Table 1), it is apparent that both specific

activity and degree of purification of the protease increased significantly compared to extracellular medium. After Octyl-sepharose CL-4B column chromatography, some of protease-1 and protease-3 were purified. Protease-1 and protease-3 did not shown very high specific activity, which could be due to the fact that some protein was denatured during the purification. However, some of protease-1 and protease-3 were in mixture with protease-2. The mixture of protease-2 and protease-3 showed a higher specific activity than purified proteases in the azocasein assay (see fraction numbers 5-8 on Figure 8) This could indicate that the mixture of proteases has some kind of cooperativeeffect or protease-2 has a higher specific activity in this azocasein assay since protease-2 is the majority of this mixture (protease-2 showed a much stronger band than protease-3 on SDS-PAGE. Gel did not show). I did not carry on with protease-2, because protease-2 was not separated by this purification process. Protease purification experiment was done many times, the date on table 1 is one time experiment results which is very close to average result.

Figure 6. Cation exchange chromatography on CM-52 cellulose of the *Xcm* filtrate by a batch process eluted with linear gradient of 0.0-1.0 M NaCl in Tris-HCl (pH 7.5) buffer. Five ml fractions were collected. Protease activities were measured by azocasein assay. Protein concentration were measured by BCA assay. The pooled fractions for proteases are 17-30.

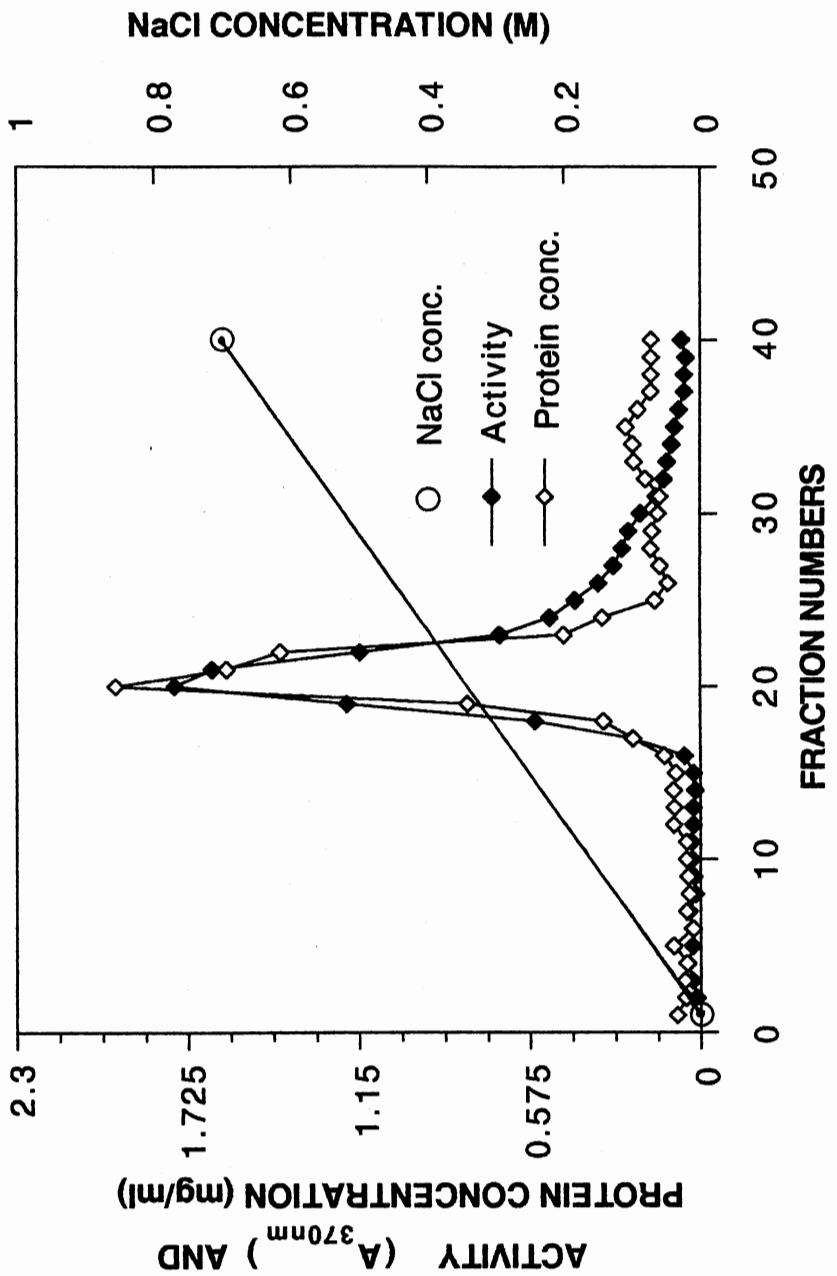
NaCl CONCENTRATION (M)
1
0.8
0.6
0.4
0.2
0
NaCl conc.
Activity
Protein conc.
2.3
1.725
1.15
0.575
0
0
10
20
30
40
50
FRACTION NUMBERS
ACTIVITY (A_{370nm}) AND
PROTEIN CONCENTRATION (mg/ml)

Figure 7. Coomassie Blue-Stained SDS-Polyacrylamide Gel showing a mixture presumally of proteases from the DEAE purification step. Lane 1, molecular weight markers [lysozyme, 14,400 (This marker did not show on this gel); soybean trypsin inhibitor, 21,500; carbonic anhydrase, 31,000; ovalbumin, 45,000; bovine serum albumin, 66,200; rabbit muscle phosphorylase, 97,400]. Lane 2, fraction from DEAE chromatography : protease-1, 29,000; protease-2, 38,000; protease-3, 43,000.

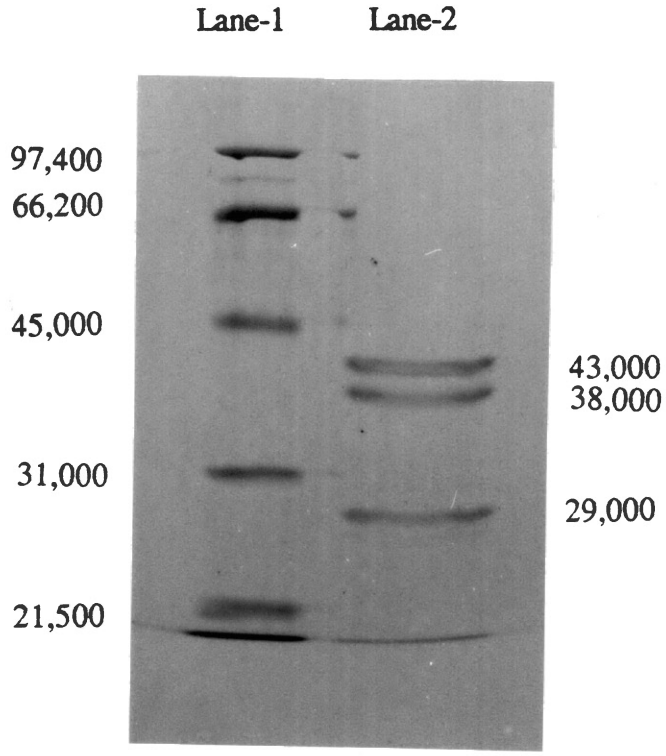
Lane-1
Lane-2
97,400
66,200
45,000
31,000
21,500
43,000
38,000
29,000

Figure 8. Purification of protease-1 and 3 by reverse phase chromatography on Octyl-Sepharose CL-4B column (20 ml). After concentration step, concentrated protease solution (20 ml) in 4.0 M NaCl was applied to the column, eluted by a step gradient of decreasing NaCl concentrations in 0.01 M Tris-HCl, pH 7.5, and two 5- ml fractions were collected at each NaCl concentration (4.0M, 3.0 M, 2.0 M, 1.0 M, 0.0 M). Protease-1 was eluted in 3 M NaCl and Protease-3 was eluted in 0.0 M NaCl. The pooled fractions for protease-1 are 3-4 and the pooled fractions for protease-3 are 9-10.

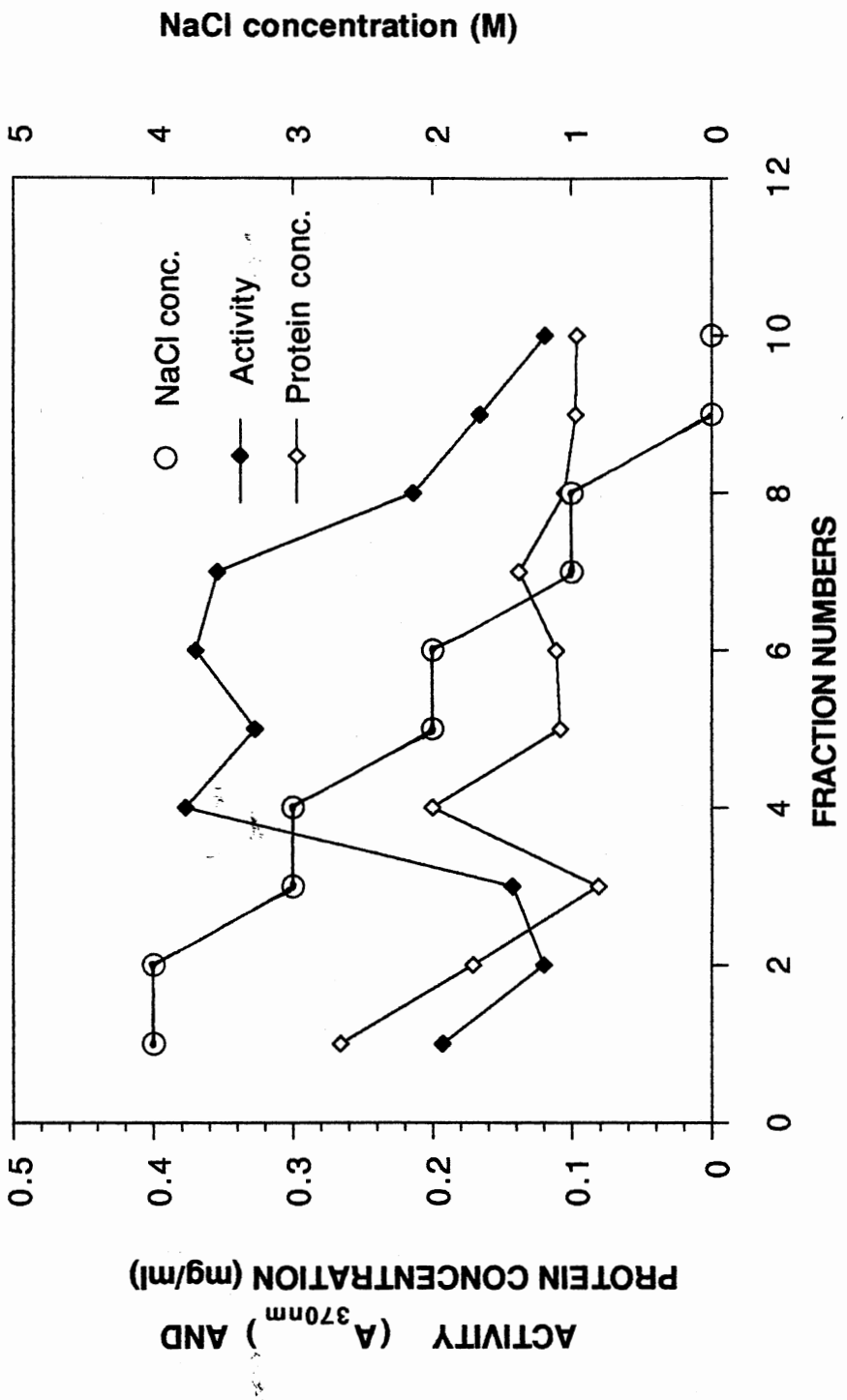
NaCl concentration (M)
5
4
3
2
1
0
NaCl conc.
Activity
Protein conc.
0.5
0.4
0.3
0.2
0.1
0
0
2
4
6
8
10
12
FRACTION NUMBERS
ACTIVITY (A_{370nm}) AND
PROTEIN CONCENTRATION (mg/ml)

TABLE 1

ISOLATION AND PURIFICATION OF TWO PROTEASES FROM *XANTHOMONAS CAMPESTRIS* PV. *MALVACEARUM*

Purification stage	Volume (ml)	Protein mg/ml	Protein Total (mg)	Activity units/ml	Activity units/mg	Activity Total	Yield (%)	Purification
Culture supernatant	2250	0.476	1071	0.556	1.168	1251	100	1
CM-52 eluate	65	0.0268	1.74	2.716	69.99	190.1	15.2	59.9
DEAE-cellulose	70	0.0222	1.55	2.48	112.0	173.6	13.8	95.9
Concentrater	20	0.0714	1.43	8.58	120.0	171.6	13.7	102.7
Sepharose eluate P-1	10	0.0141	0.141	0.52	36.8	5.2	0.41	31.57
Sepharose eluate P-3	10	0.0097	0.097	0.29	29.89	2.9	0.23	25.6

Activity units are ΔA_{370}/15min.

Figure 9. Coomassie Blue-Stained SDS-Polyacrylamide Gel showing in lane 2, protease-1 (29,000) from the mixture of fraction 3 and fraction 4 eluted from Octyl-Sepharose CL-4B column (contained 50 μg protein), and in lane 1, molecular weight markers (the same ones as in Figure 7. The marker of lysozyme, 14,400 did not show on this gel).

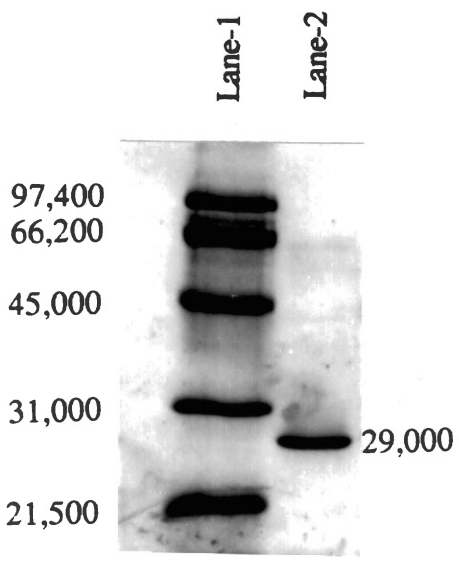
Lane-1
Lane-2
97,400
66,200
45,000
31,000
21,500
29,000

Figure 10. Coomassie Blue-Stained SDS-Polyacrylamide Gel showing in lane 1, molecular weight markers, lane 2, protease-3 (43,000) from the mixture of fraction 9 and 10 eluted from Octyl-Sepharose CL-4B column (contained 30 μg protein).

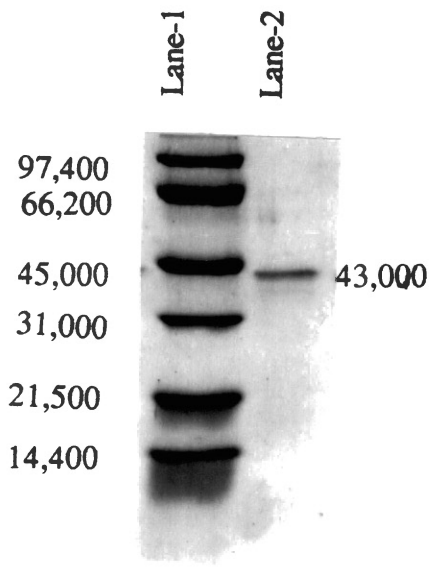
Lane-1
Lane-2
97,400
66,200
45,000
31,000
21,500
14,400
43,000

Optimum pH of Purified Protease

The pH dependence of purified proteases, protease-1 and protease-3, was investigated by using four different kinds of buffer systems in the standard reaction mixture each at 0.01 M: 2[N-Morpholino] ethanesulfonic acid (MES) (pH 5.5 to 6.5); N, N bis[2-Hydroxyethyl] 2-aminoethane-sulfonic acid (BES) (pH 6.5 to 7.5); N-[2-Hydroxyethyl] piperazine-N'-3-propanesulfonic acid (EPPS) (pH 7.5 to 8.5) and 3-[(1,1-Dimethyl-2-hydroxyethyl) amino] -2-hydroxypropanesulfonic acid (AMPSO) (pH 8.5 to 9.5). All the buffers were adjusted in pH with NaOH or HCl to the following pH's: for MES (pH 5.5, 6.0, 6.5); BES (pH 6.5, 7.0, 7.5); EPPS (pH 7.5, 8.0, 8.5); AMPSO (pH 8.5, 9.0, 9.5) and were filter sterilized. Before assay, protease solutions were dialyzed against 0.001 M Tris-HCl buffer pH 7.5 in order to remove Tris-HCl buffer. Protease-1 and protease-3 showed maximum activity for azocasein at the slightly acid-to-neutral pH range of 5.5 to 7.5 (Figure 11 and Figure 12).

Protease Inhibition and Reactivation Studies

Inhibitor Studies on Two Purified Proteases from *Xcm*

The effects of various inhibitors on the activity of protease-1 and protease-3 were assessed with azocasein substrate as described in Materials and Methods following 30 min. preincubation with various potential inhibitors (0.1 ml). For the inhibition study, azocasein was used at a lower concentration than in the routine enzyme activity assay (0.1 ml of 1% azocasein instead of 0.25 ml). *Xcm* proteases were concentrated in order to use the same volume as for trypsin and thermolysin (0.1 ml). The patterns of inhibition of the two proteases were compared with that of the serine protease trypsin and the metalloprotease thermolysin with the results shown in Table 2. Protease-1 and protease-3 are insensitive to the serine protease inhibitors PMSF and 3,4-Dichloroisocoumarin, but are inhibited by EDTA, phosphoramidone and 1,10-phenanthroline. Protease-1 activity was enhanced by

$ZnCl_2$; presumably the purified proteases did not have enough Zn^{++} to give full activity due to loss of Zn^{++} through the 10,000 M.W.cutoff membrane during the concentration step. Thermolysin was severely inhibited by the last four reagents, while trypsin, was not. This result indicates that protease-1 and protease-3 are metalloproteases and Zn^{++} ions are required for their activity.

Reactivation of the EDTA and 1,10-Phenanthroline Inactivated Proteases

Protease activity inhibited by EDTA or 1,10-phenanthroline could be reactivated by metal ions. These effects were tested at pH 7. To purified proteases (0.4 ml) preinhibited (preincubation for 30 min) by inhibitors (0.1 ml) in 0.01 M BES buffer (0.25 ml) were added 30 mM $ZnCl_2$, $MgCl_2$, or $MnCl_2$ (0.1 ml). After a 30 min preincubation at 30° C, 0.1 ml of 1% azocasein and distilled water were added up to 1 ml.

Protease-1 inhibited by EDTA or 1,10-phenanthroline was reactivated by $ZnCl_2$. In the case of 1,10-phenanthroline inhibition was also reactivated by $MnCl_2$ (Table 3). Protease-3 inhibited by EDTA or 1,10-phenanthroline were reactivated by $ZnCl_2$ slightly compared with protease-1. In the case of 1,10-phenanthroline inhibition, protease-3 was reactivated by $ZnCl_2$, $MgCl_2$ and $MnCl_2$ (Table 4). These results indicated that metal ions are required for protease-1 and protease-3 activity. This experiment was done five times for protease-1 and three times for protease-3, the data on Table 3 and Table 4 are the average results.

Figure 11. pH optimum of protease-1. Protease activity of the Protease-1 (from Octyl-sepharose column eluted with 3M NaCl in 0.01 M Tris-HCl buffer) was assayed, using 1% azocasein (A_{370nm}), as a function of pH in : 0.01 M 2[N-Morpholino] ethanesulfonic acid (MES); N,N bis [2-Hydroxyl-ethyl]2-aminoethane-sulfonic acid (BES); N-[2-Hydroxyethyl] piperazine-N'-[3-propanesulfonic acid] (EPPS) and 3-[(1.1-Dimethyl-2-hydroxyethyl) amino]-2-hydroxypropanesulfonic acid (AMPSO).

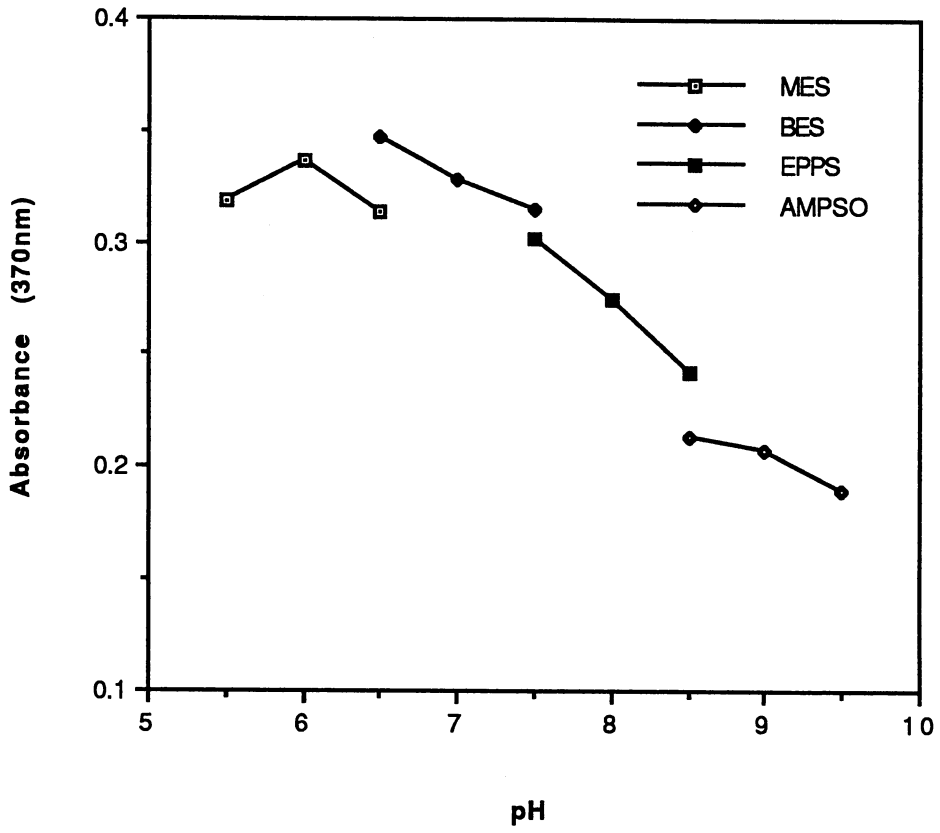
0.4
0.3
0.2
0.1
Absorbance (370nm)
5
6
7
8
9
10
pH
MES
BES
EPPS
AMPSO

Figure 12. pH optimum of protease-3. Protease activity of the protease-3 (from Octyl-sepharose column eluted with 0.01 M Tris-HCl buffer, pH 7.5)was assayed using the same method as for protease-1.

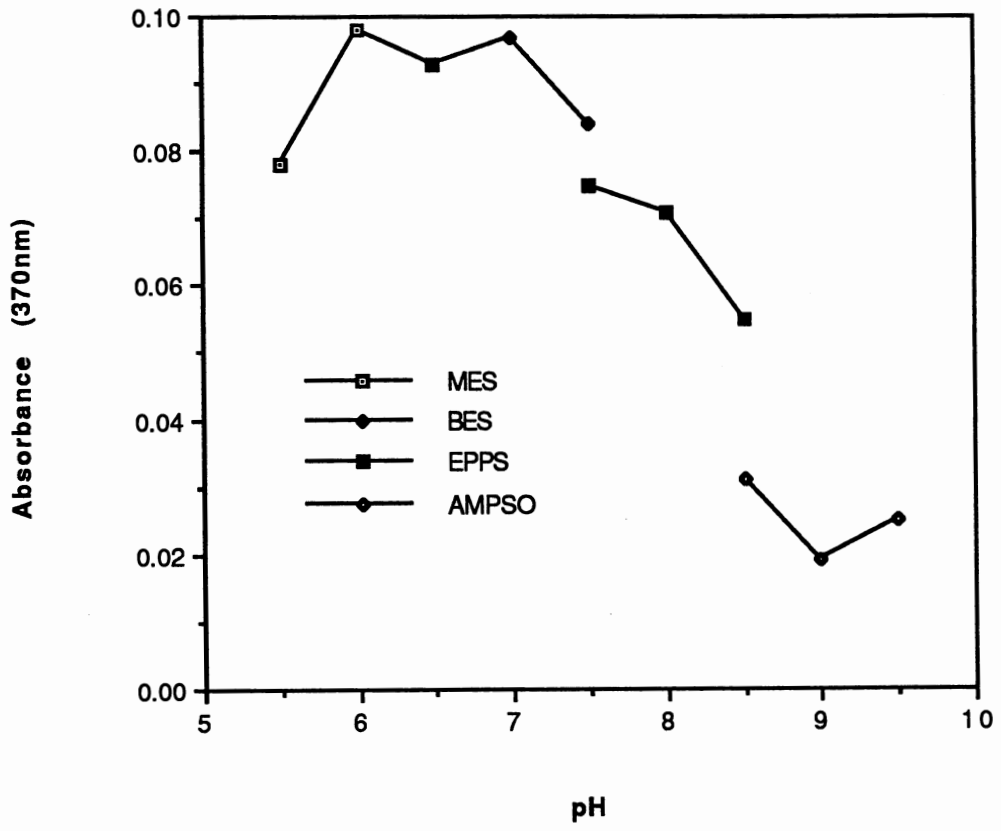
0.10
0.08
0.06
0.04
0.02
0.00
Absorbance (370nm)
5
6
7
8
9
10
pH
MES
BES
EPPS
AMPSO

TABLE 2

EFFECT OF VARIOUS POTENTIAL INHIBITORS ON ACTIVITY OF PROTEASES FROM *XANTHOMONAS CAMPESTRIS* PV. *MALVACEARUM*

Inhibitor	Concentration (mM)	% Activity Remaining			
		Xcm P-1 (0.05mg/ml)	*Xcm* P-3 (0.05mg/ml)	Trypsin (0.05mg/ml)	Thermolysin (0.011mg/ml)
None	-	100	100	100	100
3,4-Dichloroisocoumarin	0.25	108	97	26	83
PMSF	3.0	109	97	19	97
Phosphoramidone	0.1	53	24	107	13
EDTA	3.0	3	21	86	0.5
1,10-Phenanthroline	1.0	7	18	88	10
$ZnCl_2$	3.0	119	74	98	20

TABLE 3

EFFECT OF VARIOUS METALLO-IONS ON REACTIVATION OF PROTEASE-1 FROM *XANTHOMONAS CAMPESTRIS* PV. *MALVACEARUM*

Metallo-ion	% Activity Remaining		
	P-1(0.4ml of 0.025mg/ml)	P-1+EDTA (3mM)	P-1+1,10-Phenanthroline (3mM)
None	100	47	36
$ZnCl_2$ (3mM)		84	107
$MgCl_2$ (3mM)		43	39
$MnCl_2$(3mM)		15	63

TABLE 4

EFFECT OF VARIOUS METALLO-IONS ON REACTIVATION OF PROTEASE-3 FROM *XANTHOMONAS CAMPESTRIS* PV. *MALVACEARUM*

Metallo-ion	% Activity Remaining		
	P-3(0.4ml of 0.025mg/ml)	P-3+EDTA (3mM)	P-3+1,10-Phenanthroline (3mM)
None	100	2	6
$ZnCl_2$ (3mM)		14	21
$MgCl_2$ (3mM)		3	38
$MnCl_2$(3mM)		8	29

Peptide Bond Specificity

The peptide bond cleavage specificities of *Xcm* proteases were studied using oxidized insulin A chain, oxidized insulin B chain, glucagon and Thymopoietin II Fragment 32-36. The complete sequences of these peptides are shown on Figure 23. The peptide fragments generated by protease cleavage of these substrates were subjected to either Liquid Secondary Ion Mass Spectroscopy or Electrospray Mass Spectrometry.

Peptide Bond Specificity of Protease-1

Peptide bond specificity of protease-1 was investigated with oxidized insulin B chain, oxidized insulin A chain, glucagon and Thymopoietin II Fragment 32-36. The substrates (20µl of 1 mg/0.15ml 0.01 M NH_4OH and 20µl of 0.01 M Tris-HCl buffer pH 7.5) were digested with the purified protease-1 (30µl of 1 mg/ml) from *Xcm* for one hour at 30° C. It is presumed that protease-1 has two cleavage sites on insulin B chain (Figure 23) (N-terminal to the cysteic acids) based on Gholson and Roberts unpublished results. Chromatography of the protease-1 digested oxidized insulin B chain on reverse phase HPLC is shown in Figure 13; peaks 1, 2, 3, and 4 eluted earlier than the undigested insulin B chain from this column, indicating that the B chain had been cleaved into smaller peptides. The LSIMS spectrum of this digestion is shown in Figure 14. A mass of 757 is consistent with the molecular weight plus a proton [$M+H^+$] of the peptide F-V-N-Q-H-L, which was peak-1 on Figure 13 since this peak was collected from HPLC and independently identified by LSIMS. Masses of 779 and 801 are consistent with [$M+Na^+$] and [$M+2Na^+$] of the above peptide, respectively. The four peaks, 1, 2, 3, and 4, separated in the reverse phase HPLC are the peptides of F-V-N-Q-H-L, C-G-E-R-G-F-F-Y-T-R-K-A, C-G-S-H-L-V-E-A-L-Y-L-V and F-V-N-Q-H-L-C-G-S-H-L-V-E-A-L-Y-L-V, respectively (based on the observation that when incubation time was longer, peak-4 decreased and peak-1 and peak-3 increased). Since F-V-N-Q-H-L is the only peptide with a mass of 757 that can be

generated from oxidized insulin B chain, finding its mass by LSIMS confirms the predicted cleavage site.

Protease-1 has three cleavage sites on insulin A chain (Figure 23) based on unpublished results of Gholson and Roberts. Chromatography of the protease-1 digested oxidized insulin A chain on reverse phase HPLC is shown in Figure 15. Seven major peaks were produced from this digestion. Two peptide fragments were identified by LSIMS (Figure 16). Masses of 545, 567, 589, and 611 were from $[M+H^+]$, $[M+Na^+]$, $[M+2Na^+]$ and $[M+3Na^+]$ respectively of peptide C-Y-V-E-Q. Masses of 1203, 1225, and 1247 were consistent with $[M+Na^+]$, $[M+2Na^+]$ and $[M+3Na^+]$ respectively of peptide $C(SO_3H)$-S-L-Y-Q-L-E-N-Y (Other masses are ether from matrix or contaminant). I hypothesize the seven peaks from oxidized insulin A chain are as follows: peak-1 is C-N and peak-2 is C-C-A-S-V (according to peptide size and polarity of side chains), peak-3 is G-I-V-E-Q (according to M.W. from eletrospray ionization mass spectrum of the individual peak), peak-4 is G-I-V-E-Q-C-C-A-S-V and peak-5 is C-C-A-S-V-C-S-L-Y-Q-L-E-N-Y (according to peptide size and polarity of side chain), peak-6 is C-S-L-Y-Q-L-E-N-Y (according to M.W. from eletrospray mass spectrum of the individual peak), and peak-7 is oxidized insulin A chain (compared to the control). Since cysteic acid with its strong negative charge is difficult to ionize, some peptides with multiple cysteic acids did not show up in the spectrum of LSIMS.

Since cysteic acid is not a normal constituent of proteins, it was assumed that the natural cleavage site of *Xcm* protease-1 is next to an amino acid residue with size and charge characteristics similar to cysteic acid. Aspartic acid, an amino acid which is not present in either the insulin A chain or B chain, resembles cysteic acid both in size and charge. Therefore glucagon, a 29-amino-acid peptide containing three aspartic acid residues and Thymopoietin II Fragment 32-36, a five amino acid peptide containing one aspartic acid residue were tested. In both cases, the fragments separated by HPLC (Figure 17 and Figure 21) and the identification with LSIMS for glucagon (Figure 18, 19, 20) and

electrospray MS for the Thymopoietin II Fragment 32-36 (Figure 22) indicated that these peptides were cleaved only on the N-terminal side of aspartic acid residue.

Protease-1 has three cleavage sites on glucagon (Figure 23) based on Gholson and Roberts unpublished results. Five peptide fragments were generated by protease-1 digestion of glucagon, three of them were separated on the reverse phase HPLC individually. All five peptides was identified by LSIMS; peptide D-S-R-R-A-Q was shown in LSIMS spectrum as 732 [M+H^+] and 754 [M+Na^+], peptide D-Y-S-K-Y-L (peak-2 according to M.W. from eletrospray mass spectrum of the individual peak) was shown in LSIMS spectrum as 788 [M+H^+], 810 [M+Na^+], and 832 [M+2Na^+], peptide H-S-Q-G-T-F-T-S (peak-1 according to M.W. from eletrospray mass spectrum of the individual peak) was shown in LSIMS spectrum as 864 [M+H^+] and 886 [M+Na^+], (Figure 18), peptide D-F-V-Q-W-L-M-N-T was shown in LSIMS spectrum as 1154 [M+H^+], 1175 [M+Na^+], 1198 [M+2Na^+], and 1220 [M+3Na^+] (Figure 19); peptide D-S-R-R-A-Q-D-F-V-Q-W-L-M-N-T was shown in LSIMS spectrum as 1868 [M+H^+], 1890 [M+Na^+] and 1912 [M+2Na^+] (Figure 20).

Protease-1 has one cleavage site on Thymopoietin II Fragment 32-36 based on Gholson and Roberts unpublished results. Two peptide fragments generated by protease-1 digestion of Thymopoietin II Fragment 32-36 were separated on the reverse phase HPLC individually (Figure 21). Peak-1 was identified to be the peptide R-K which was shown in ESIMS as 303.0 [M+H^+]. Peak-2 was identified to be the peptide D-V-Y which was shown in ESIMS as 396.0 [M+H^+], 418.0 [M+Na^+] 440.0 [M+2Na^+] and 462.0 [M+3Na^+]. Peak 3 was identified to be the undigested whole peptide R-K-D-V-Y which was shown in electrospray mass spectrum as 680.0 [M+H^+], 702.0 [M+Na^+], 716.0 [M+2NH_4^+], 738.0 [M+2NH_4^++Na^+] and 760.0 [M+2NH_4^++2Na^+] (Figure 22).

The above results indicated that both oxidized insulin A chain and B chain were cleaved by protease-1 only on the N-terminal side of cysteic acid residue and both glucagon and thymopoietin II Fragment 32-36 were cleaved by protease-1 only on the N-terminal

side of aspartic acid residue. The peptide bond specificity of protease-1 was also tested by different incubation times (30 min, 1 h and 4 h) with insulin B chain (data not shown), the specificity of protease-1 had not changed. Therefore, it is summarized that protease-1 only cleaves the N-terminal side of aspartic acid (Figure 23).

Peptide Bond Specificity of Protease-3

Peptide bond specificity of protease-3 was determined by reverse phase HPLC and ESIMS with glucagon, oxidized insulin B chain and A chain as the substrate.

Protease-3 cleavage sites on the tested substrates were unknown. At least seven new peptide fragments from glucagon were shown on HPLC chromatography (Figure 25). The peptide fragments as a mixture and each of the seven single peak fractions from HPLC were subjected to ESIMS. Most fragments were identified. The ESIMS result for the peptide mixture is shown in Figure 26, eight signals corresponded to the listed peptides (Figure 24) generated from glucaon digested by protease-3. Masses of 257.0 and 301.0 are as predicted for $[M+NH_4^+ + Na^+]$ and $[M+NH_4^+ + 3\ Na^+]$ respectively for the peptide A-Q. Masses of 354.0 and 376.0 are as predicted for $[M+H^+]$ and $[M+Na^+]$ respectively for the peptide F-T-S and also predicted for $[M+Na^+]$ and $[M+2\ Na^+]$ respectively for the peptide L-D-S. Masses of 478.0 and 500.0 are as predicted for $[M+H^+]$ and $[M+Na^+]$ respectively for the peptide L-M-N-T. Mass of 529.0 is as predicted for $[M+H^+]$ for the peptides H-S-Q-G-T and R-R-A-Q. Masses of 579.0 and 601.0 are as predicted for $[M+H^+]$ and $[M+Na^+]$ respectively for the peptide F-V-Q-W. Mass of 673.0 is as predicted for $[M+H^+]$ for the peptide D-Y-S-K-Y. Masses of 694.0 and 716.0 are as predicted for $[M+H^+]$ and $[M+Na^+]$ respectively for the peptide D-F-V-Q-W. Masses of 788.5 and 810.0 are as predicted for $[M+H^+]$ and $[M+Na^+]$ respectively for peptide D-Y-S-K-Y-L. For the ESIMS results for the individual peaks, five signals corresponded to the peptides from peaks 2, 3, 5, 6 and 7 (Figures are not shown). Therefore, I hypothesize the eight peaks from glucagon are as follows: peak-1 is A-Q, L-D-S plus R-R, peak-4 is H-S-

Q-G-T (according to peptide size and polarity of side chains), peak-2 is F-T-S, peak-3 is L-M-N-T and R-R-A-Q, peak-5 is D-Y-S-K-Y and D-Y-S-K-Y-L, peak-6 is F-V-Q-W and peak-7 is D-F-V-Q-W (according to M.W. from eletrospray mass spectrum of the individual peak), peak-8 is uncleaved glucagon. Protease-3 has nine cleavage sites on glucagon and only on the N-terminal side of aspartic acid, phenylalanine, leucine, alanine and arginine (Figure 24).

The expected masses for nine peptides from protease-3 digestion of oxidized insulin B chainwere shown on ESIMS (Figure 28). Mass of 295 is as predicted for $[M+H^+]$ for the peptide L-Y. Mass of 364 is as predicted for $[M+H^+]$ for the peptide A-L-Y. Masses of 384 and 408 are as predicted for $[M+Na^+]$ and $[M+2Na^+]$ respectively for the peptide L-V-E. Masses of 431 and 453 are as predicted for $[M+H^+]$ and $[M+Na^+]$ respectively for the peptide L-V-E-A. Mass of 552 is as predicted for $[M+H^+]$ for the peptide C-G-E-R-G. Masses of 564 and 586 are as predicted for $[M+H^+]$ and $[M+Na^+]$ respectively for the peptide L-C-G-S-H. Masses of 644 and 666 are as predicted for $[M+H^+]$ and $[M+Na^+]$ respectively for the peptide F-V-N-Q-H. Mass of 726 is as predicted for $[M+NH_4^+]$ for peptide L-V-E-A-L-Y. Mass of 803 is as predicted for $[M+H^+]$ for the peptide F-F-Y-T-P-K. Protease-3 has ten cleavage sites on oxidized insulin B chain (Figure 27).

The expected masses for five peptides from insulin A chain were shown on ESIMS (Figure 30). Mass of 257 is as predicted for $[M+H^+]$ for the peptide C-S. Masses of 278 and 301 are as predicted for $[M+H^+]$ and $[M+Na^+]$ respectively for the peptide A-S-V. Masses of 359 and 381 are as predicted for $[M+H^+]$ and $[M+Na^+]$ respectively for the peptide C-C. Masses of 425 and 462 are as predicted for $[M+H^+]$ and $[M+2NH_4^+]$ respectively for the peptide L-Y-Q. Mass of 541 is as predicted for $[M+3NH_4^+]$ for the peptide L-E-N-Y. Protease-3 has six cleavage sites on oxidized insulin A chain (Figure 29).

The above results indicate that protease-3 shows unusual peptide bond specificity cleaving on the N-terminal side of aspartic acid, phenylalanine, leucine, alanine and arginine

(five different kinds of amino acids) (Figure 31). However, it is hard to summarize what kind of protease it is. It is possible that protease-3 may be a mixture with another of the same M.W. since it showed a single band on SDS PAGE.

The mixture of protease-2 and protease-3 was also studied with oxidized insulin B chain. The HPLC spectrum of the mixture of protease-2 (majority in the mixture) and protease-3 digestion of insulin B chain is nearly identical with the HPLC spectrum of protease-3 digestion (Figure 32). This suggests that protease-2 may be derived from protease-3 by protein processing or by proteolytic cleavage during isolation.

Figure 13. Chromatography on a C_{18}-reverse phase HPLC column (4.6 X 250 mm) of a peptide mixture from *Xcm* protease-1 digestion of oxidized insulin B chain. Peak-1 is F-V-N-Q-H-L, peak-2 is C-G-E-R-G-F-F-Y-T-P-K-A, peak-3 is C-G-S-H-L-V-E-A-L-Y-L-V, and peak-4 is F-V-N-Q-H-L-C-G-S-H-L-V-E-A-L-Y-L-V.

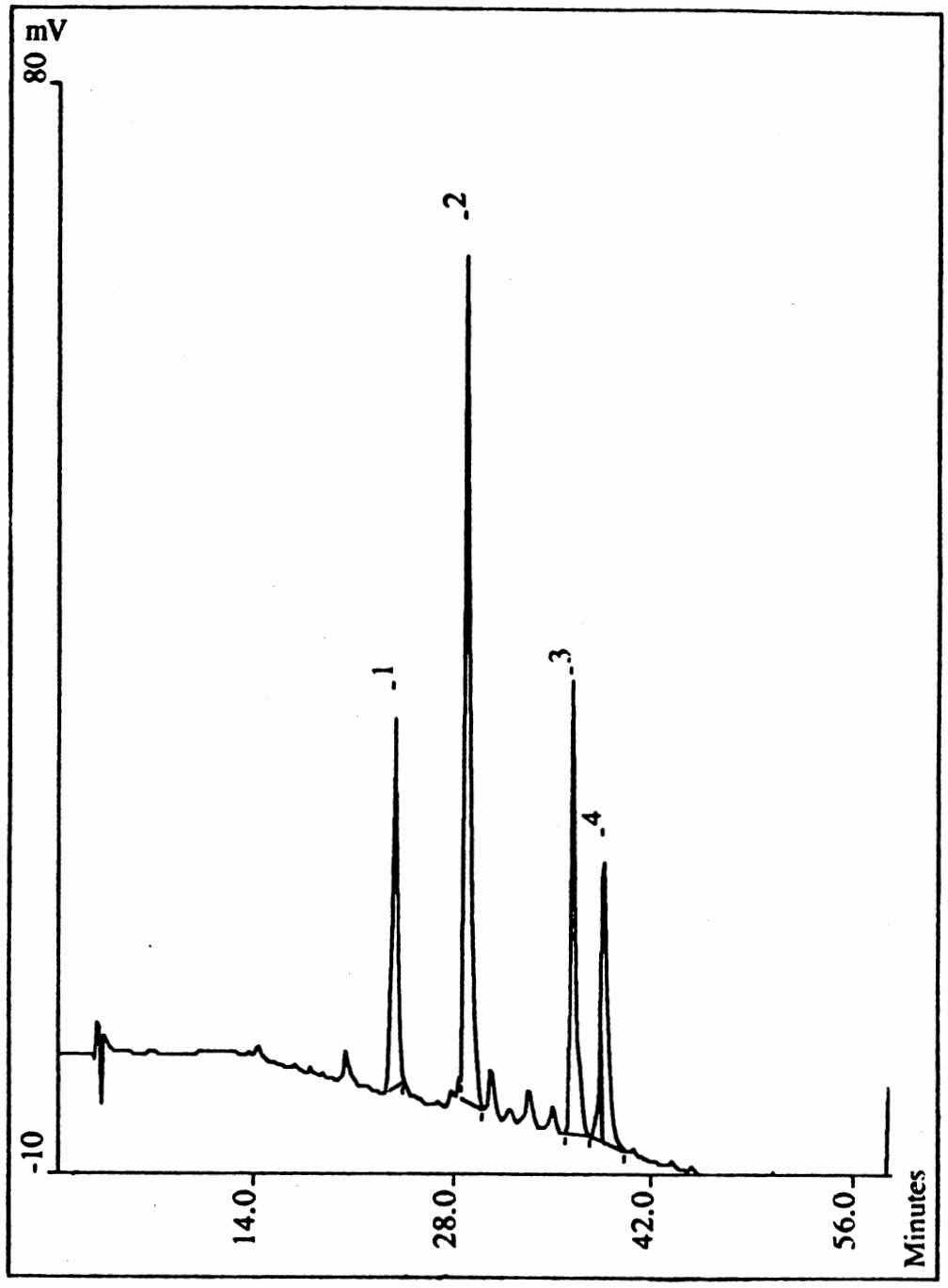
mV
80
-10
-1
-2
-3
-4
14.0
28.0
42.0
56.0
Minutes
ABSORBANCE (214nm)
RETENTION TIME

Figure 14. LSIMS spectrum of the peptide mixture obtained by *Xcm* protease-1 cleaving insulin B chain. Masses of 757, 779 and 801 are as predicted for $[M+H^+]$, $[M+Na^+]$ and $[M+2Na^+]$ respectively for the peptide of F-V-N-Q-H-L (Peak-1 on Figure 13). Others did not show (see results and discussion).

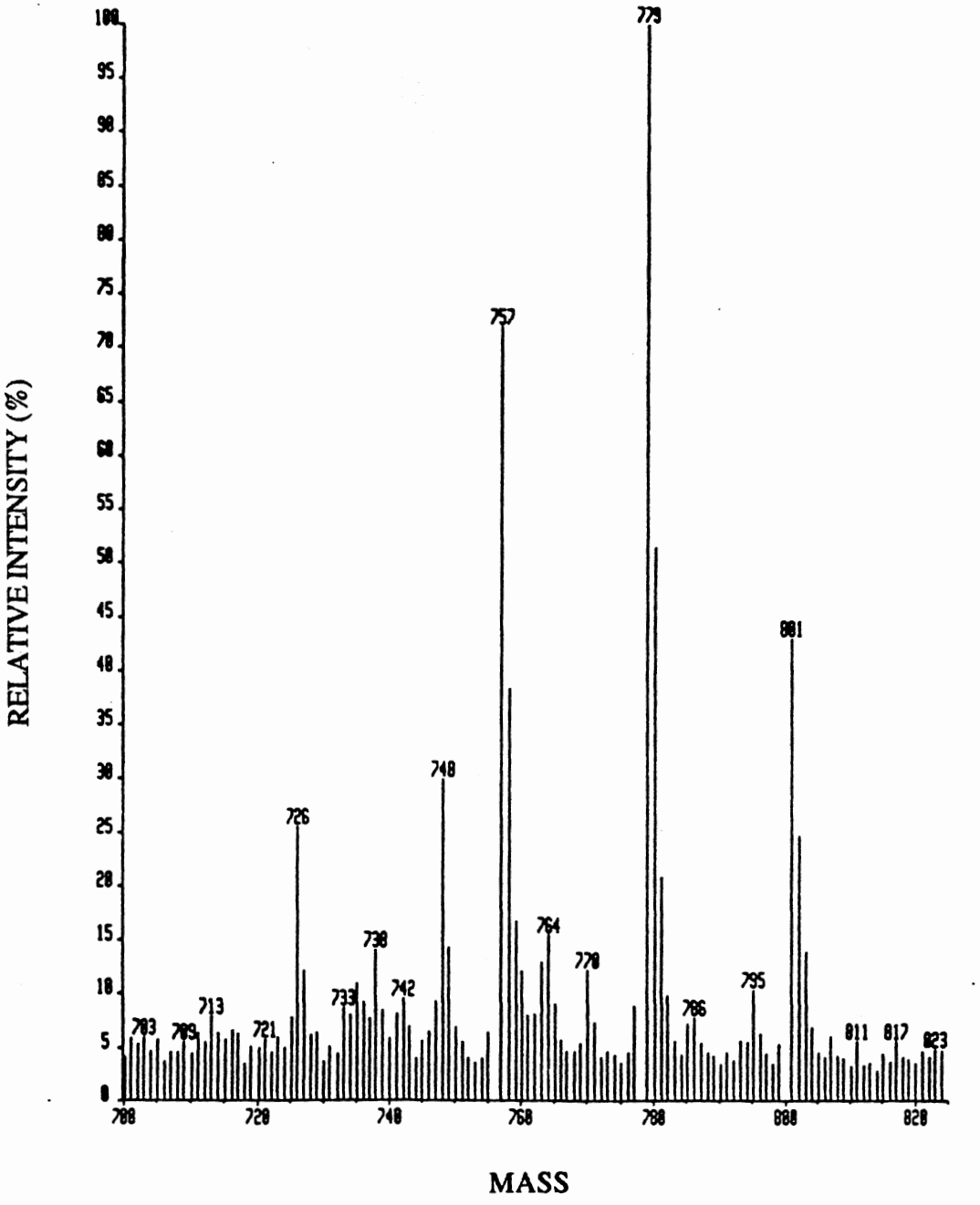
RELATIVE INTENSITY (%)
MASS
779
757
726
748
738
764
770
733
742
713
795
881
786
703
709
721
811
817
823

Figure 15. Chromatography on a C_{18}-reverse phase HPLC column of a peptide mixture from *Xcm* protease-1 digestion of oxidized insulin A chain. Peak-1 is C-N, peak-2 is C-C-A-S-V, peak-3 is G-I-V-E-Q, peak-4 is G-I-V-E-Q-C-C-A-S-V, peak-5 is C-C-A-S-V-C-S-L-Y-Q-L-E-N-Y, peak-6 is C-S-L-Y-Q-L-E-N-Y, peak-7 is uncleaved oxidized insulin A chain. Masses for the peptides G-I-V-E-Q and C-S-L-Y-Q-L-E-N-Y were indentified by LSIMS (Figure 17).

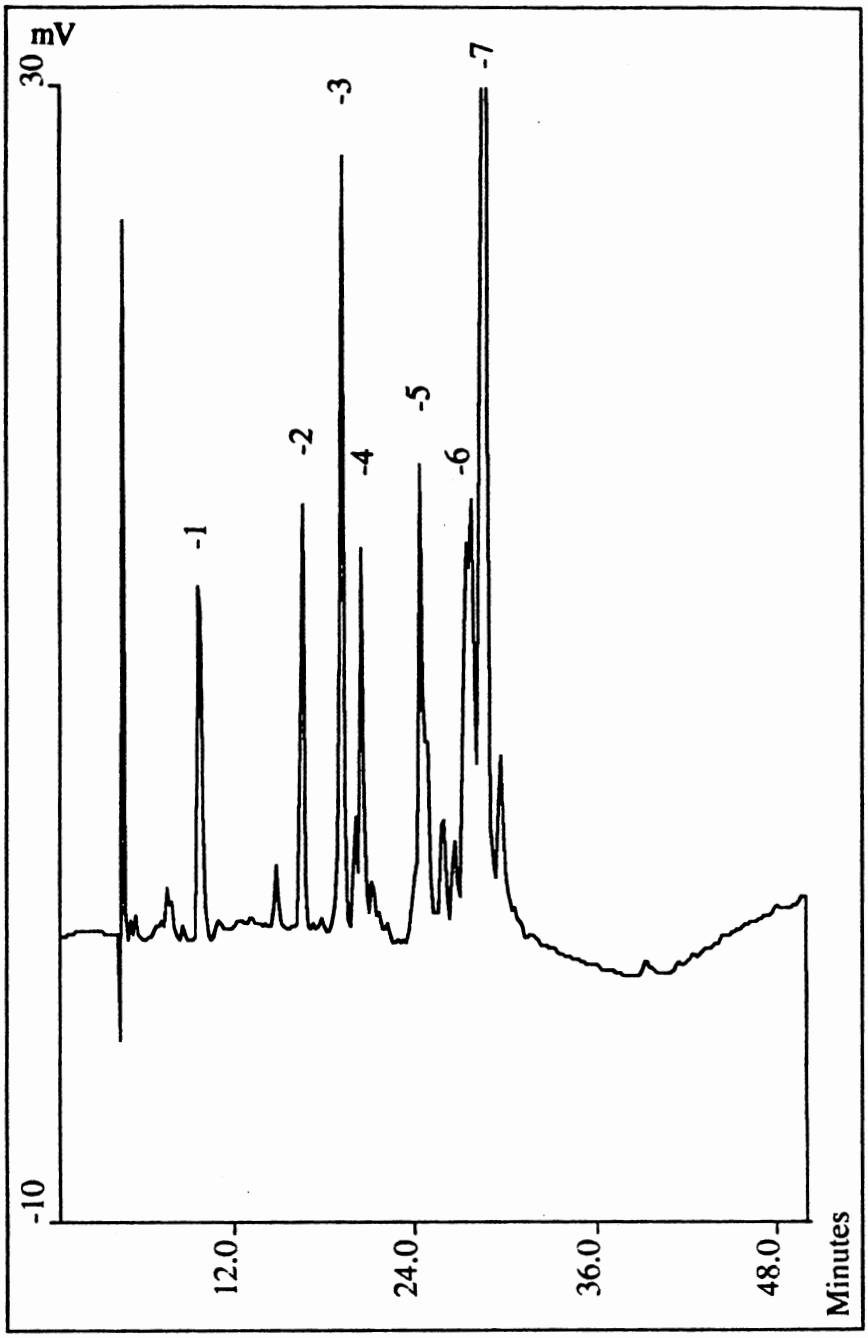
mV
30
-10
-1
-2
-3
-4
-5
-6
-7
12.0
24.0
36.0
48.0
Minutes
ABSORBANCE (214nm)
RETENTION TIME

Figure 16. LSIMS spectrum of the peptides obtained by *Xcm* protease-1 cleavage of oxidized insulin A chain. Masses of 545, 567, 589 and 611 are as predicted for $[M+H^+]$, $[M+Na^+]$, $[M+2Na^+]$ and $[M+3Na^+]$ respectively for the peptide of G-I-V-E-Q (peak-3 on Figure 15). Masses of 1203,1225 and 1247 are as predicted for $[M+Na^+]$, $[M+2Na^+]$ and $[M+3Na^+]$ respectively for the peptide of $C(SO_3H)$-S-L-Y-Q-L-E-N-Y (peak-6 on Figure 15).


RELATIVE INTENSITY (%)
MASS

Figure 17. Chromatography on a C_{18}-reverse phase HPLC column of a peptide mixture from *Xcm* protease-1 digestion of glucagon. Peak-1 is H-S-Q-G-T-F-T-S, peak-2 is D-Y-S-K-Y-L, peak-3 is D-S-R-R-A-Q, peak-4 is D-F-V-Q-W-L-M-N-T, peak-5 is D-S-R-R-A-Q-D-F-V-Q-W-L-M-N-T. Masses for all five peptides were identified by LSIMS.

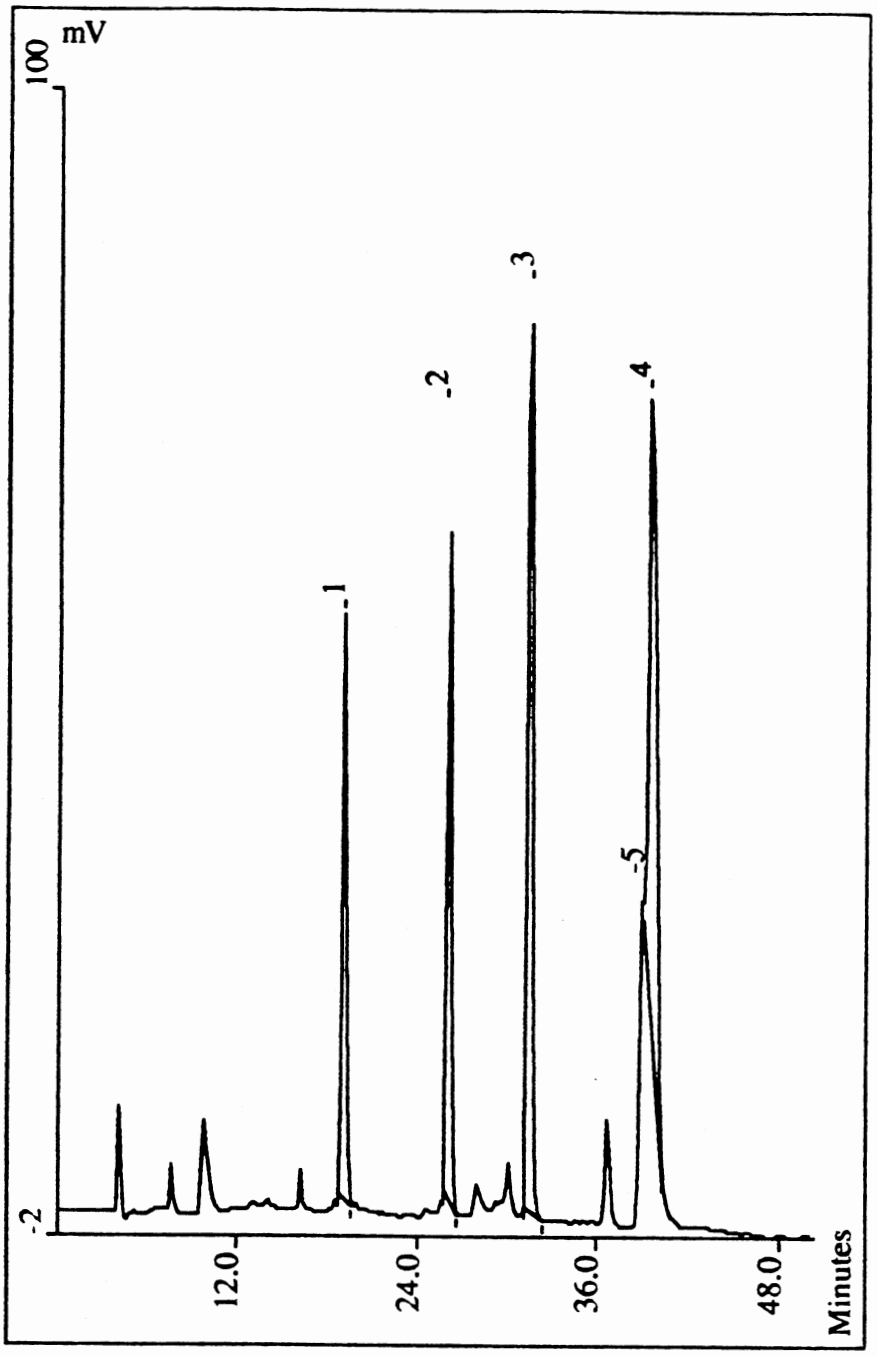
100 mV
-2
-1
-2
-3
-4
-5
12.0
24.0
36.0
48.0
Minutes
ABSORBANCE (214nm)
RETENTION TIME

Figure 18. LSIMS spectrum of the peptides obtained by *Xcm* protease-1 cleavage of glucagon. Masses of 732 and 754 are as predicted for $[M+H^+]$ and $[M+Na^+]$ respectively for the peptide D-S-R-R-A-Q (Peak-3 on Figure 17). Masses of 788, 810 and 832 are as predicted for $[M+H^+]$, $[M+Na^+]$ and $[M+2Na^+]$ respectively for the peptide D-Y-S-K-Y-L (Peak-2 on Figure 17). Masses of 864 and 886 are as predicted for $[M+H^+]$ and $[M+Na^+]$ respectively for the peptide H-S-Q-G-T-F-T-S (Peak-1 on Figure 17).

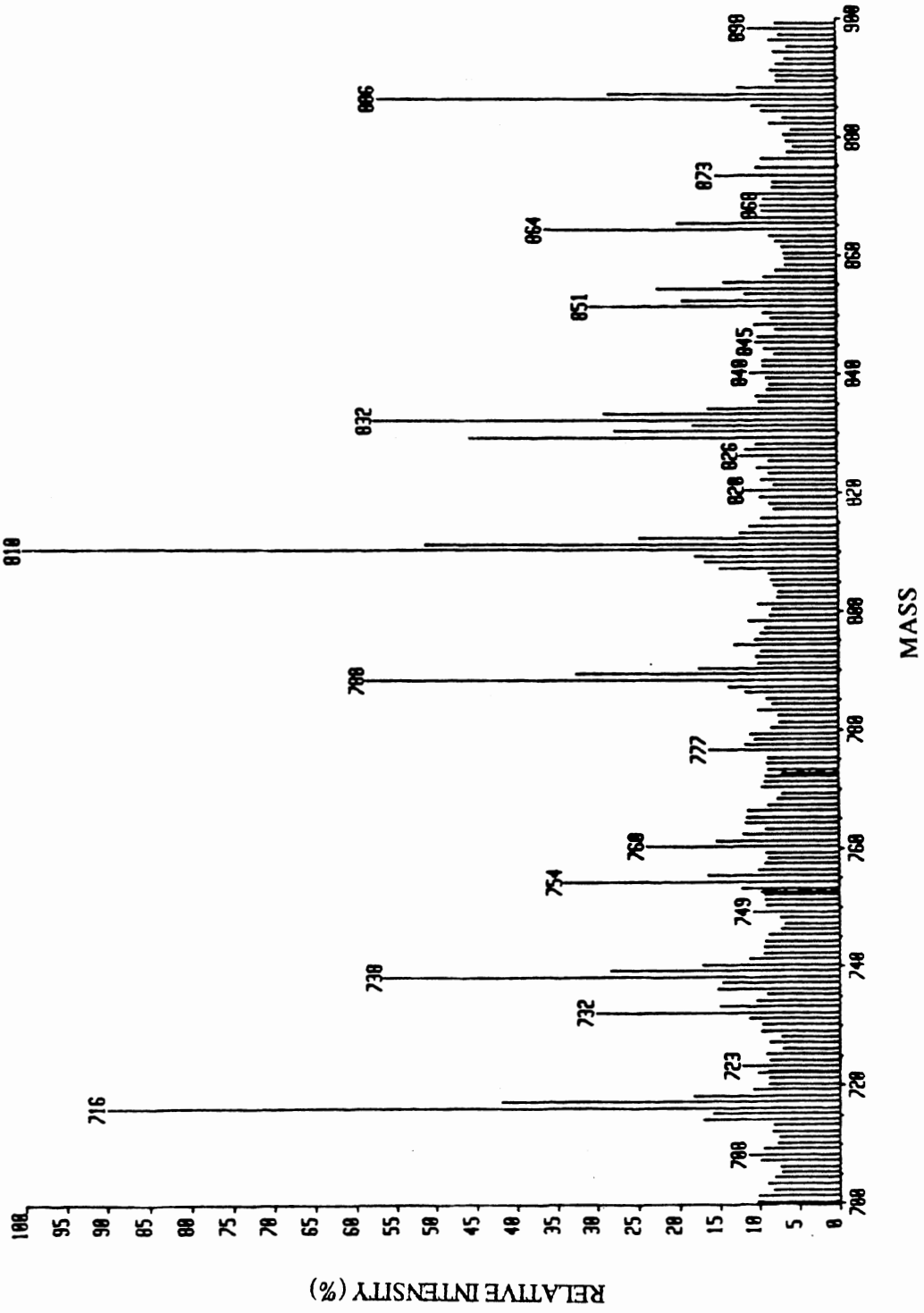
RELATIVE INTENSITY (%)
MASS
100
95
90
85
80
75
70
65
60
55
50
45
40
35
30
25
20
15
10
5
0
700
720
740
760
780
800
820
840
860
880
900
716
738
732
723
754
749
768
777
788
810
832
826
820
840
845
851
864
873
906
890

Figure 19. A continuation of the LSIMS spectrum of Figure 18. Masses of 1153, 1175, 1197 and 1219 are as predicted for $[M+H^+]$, $[M+Na^+]$ $[M+2Na^+]$ and $[M+3Na^+]$ respectively for the peptide D-F-V-Q-W-L-M-N-T (Peak-4 on Figure 17).

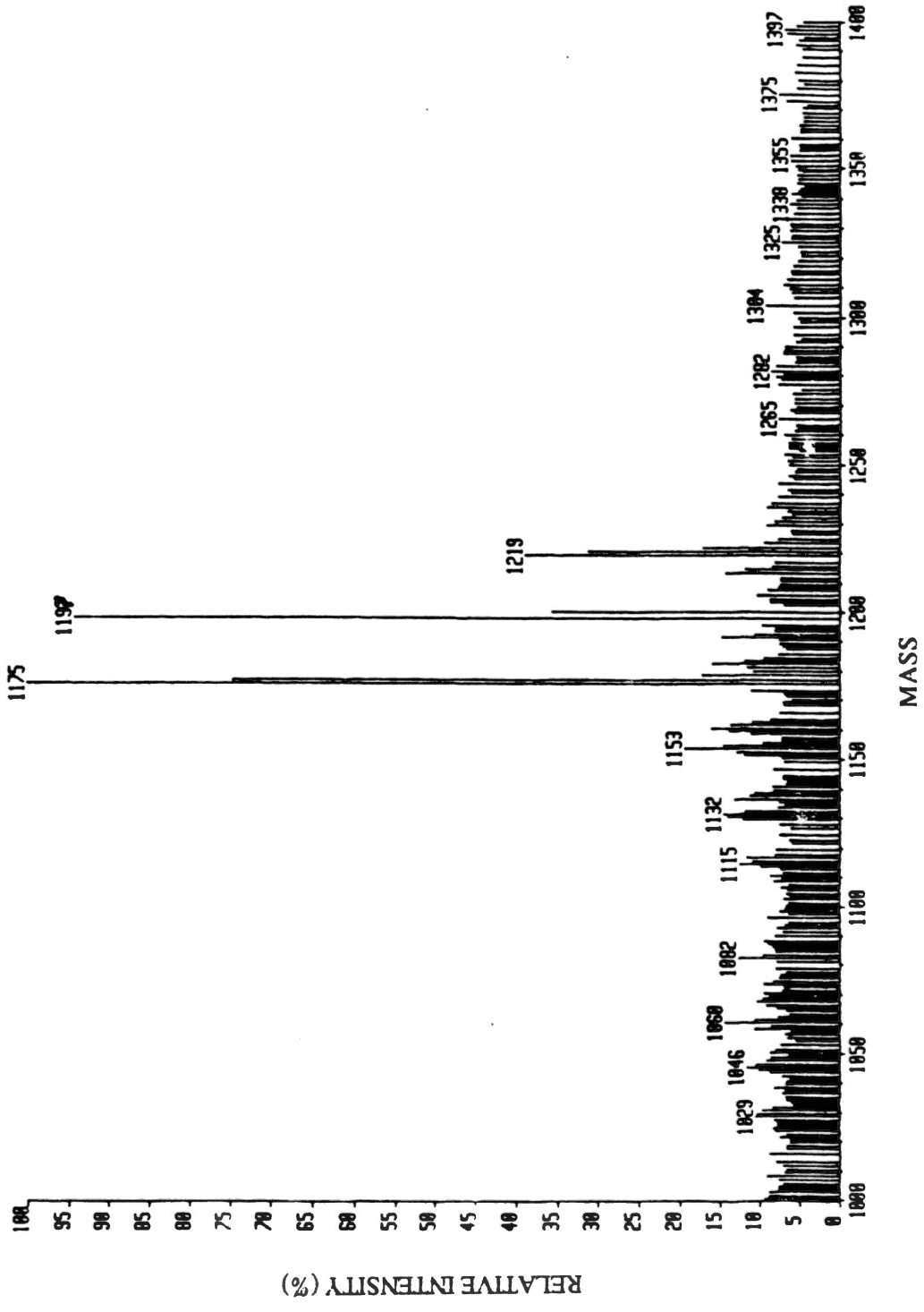
RELATIVE INTENSITY (%)
MASS
1175
1153
1219
1265
1384
1375
1397

Figure 20. A continuation of the LSIMS spectrum of Figure 19. Masses of 1868,1890, 1912 and 1933 are as predicted for $[M+H^+]$, $[M+Na^+]$, $[M+2Na^+]$ and $[M+3Na^+]$ respectively for the peptide D-S-R-R-A-Q-D-F-V-Q-W-L-M-N-T (Peak-5 on Figure 17).

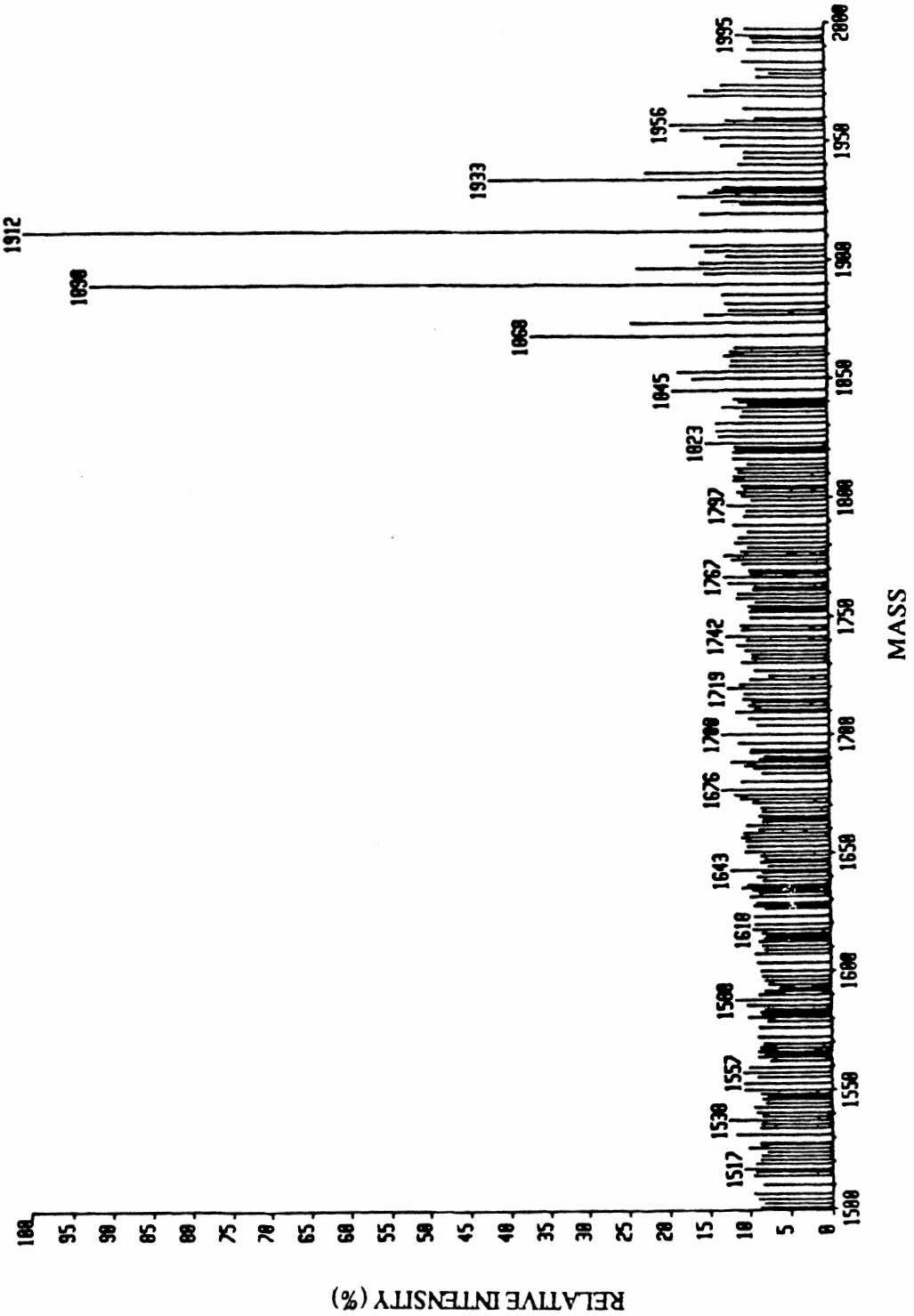
RELATIVE INTENSITY (%)
MASS
1912
1933
1956
1995
1517
1538
1557
1643
1676
1719
1742
1767
1797
1823
1845
1868
1890

Figure 21. Chromatography on a C_{18}-reverse phase HPLC column of the peptide mixture from *Xcm* protease-1 digestion of Thymopoietin II Fragment 32-36. Peak-1 is R-K, peak-2 is D-V-Y and peak-3 is R-K-D-V-Y undigested Thymopoietin II Fragment 32-36.

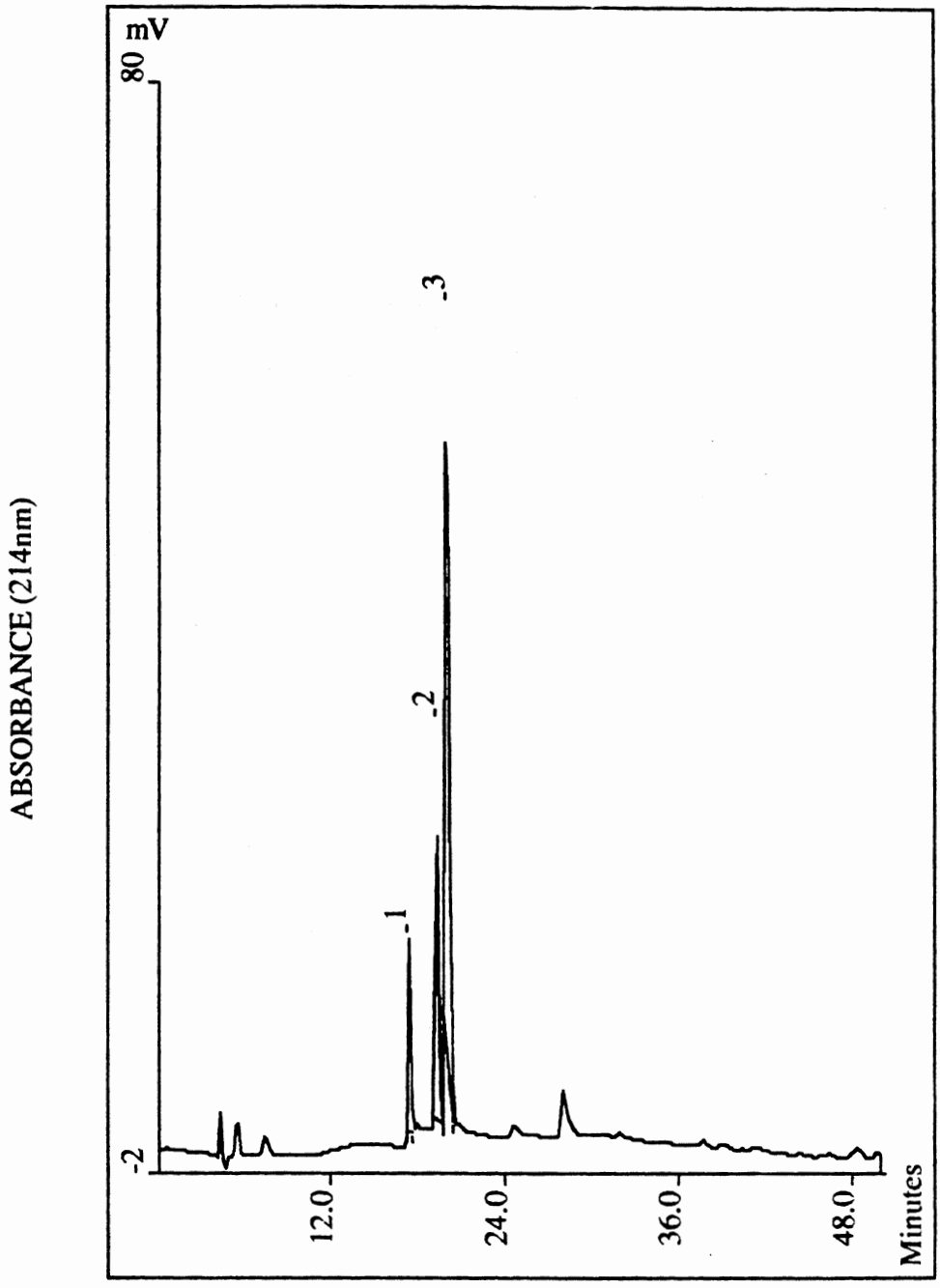
mV
80
-2
-1
-2
-3
12.0
24.0
36.0
48.0
Minutes
ABSORBANCE (214nm)
RETENTION TIME

Figure 22. Electrospray mass spectrum of the peptides obtained by *Xcm* protease-1 cleavage of Thymopoietin II Fragment 32-36. Mass of 303.0 is as predicated for $[M+H^+]$ for R-K (Peak-1 on Figure 21). Masses of 396.0, 418.0, 440.0 and 462.0 are as predicted for $[M+H^+]$, $[M+Na^+]$, $[M+2Na^+]$ and $[M+3Na^+]$ respectively for D-V-Y (Peak-2 on Figure 21). Masses of 680.0, 702.0, 716.0, 738.0 and 760.0 are as predicted for $[M+H^+]$ and $[M+Na^+]$, $[M+2NH_4^+]$, $[M+2NH_4^++Na^+]$ and $[M+2NH_4^++2Na^+]$ respectively for R-K-D-V-Y (Peak-3 on Figure 21).

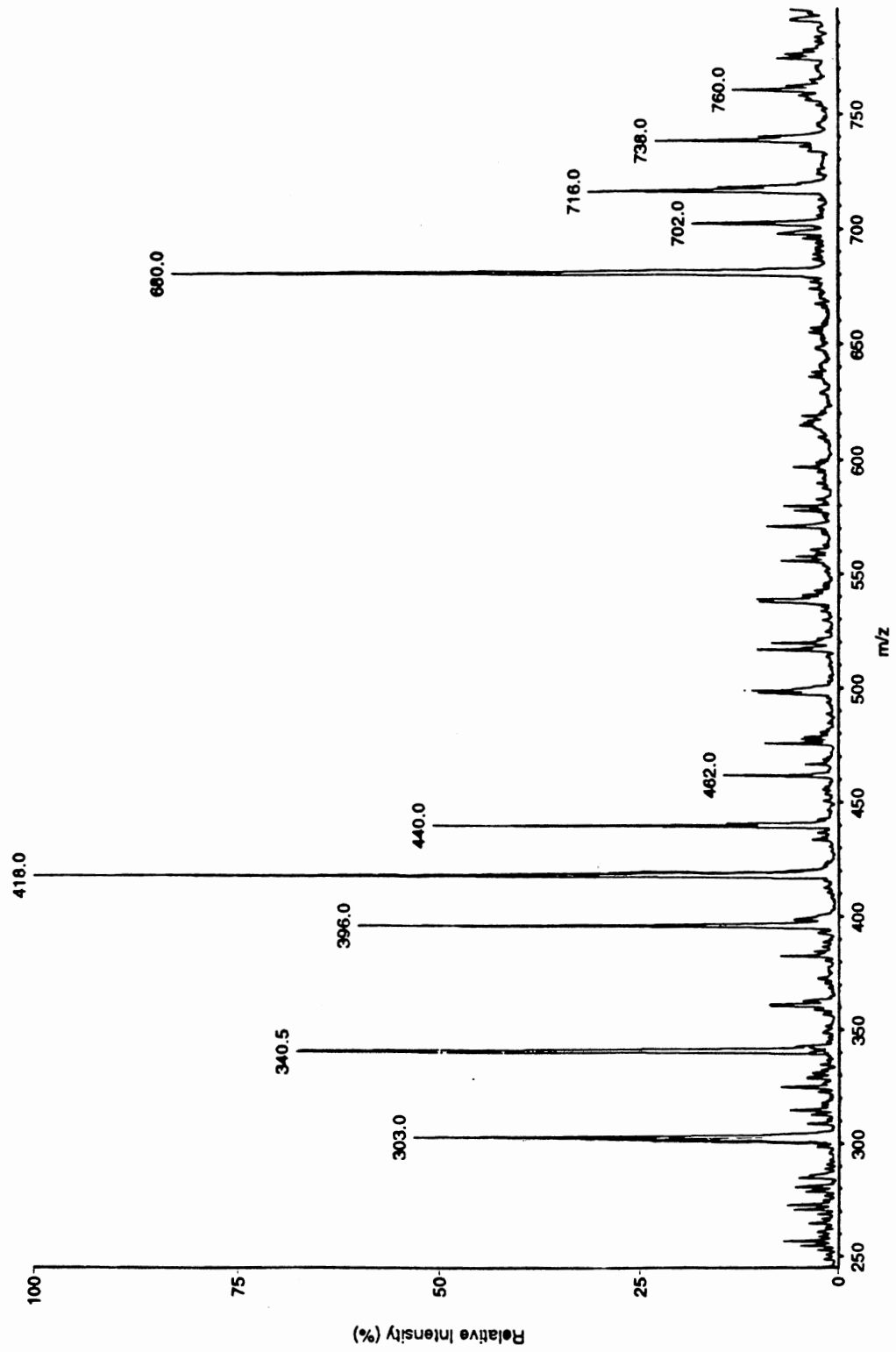
Relative Intensity (%)
100
75
50
25
0
250
300
350
400
450
500
550
600
650
700
750
m/z
680.0
716.0
738.0
760.0
702.0
418.0
440.0
462.0
396.0
340.5
303.0

Figure 23. Peptide bond specificity of protease-1 was tested with oxidized insulin B chain, oxidized insulin A chain, glucagon and Thymopoietin II Fragment 32-36. The purified protease-1 cleaved oxidized insulin A and B chains at the N-terminal side of cysteine residues which had been oxidized to cysteic acid, and cleaved glucagon and Thymopoietin II Fragment 32-36 at the N-terminal side of aspartic acid. The under lines show the peptides indentified by ESIMS.

PEPTIDE BOND SPECIFICITY OF PROTEASE-1

OXIDIZED INSULIN B CHAIN

F-V-N-Q-H-L-v-C(SO_3H)-G-S-H-L-V-E-A-L-Y-L-V-v-C(SO_3H)-G-E-R-G-F-F-Y-T-P-K-A

OXIDIZED INSULIN A CHAIN

G-I-V-E-Q-v-C(SO_3H)-C(SO_3H)-A-S-V-v-C(SO_3H)-S-L-Y-Q-L-E-N-Y-v-C(SO_3H)-N

GLUCAGON

H-S-Q-G-T-F-T-S-v-D-Y-S-K-Y-v-L-D-S-R-R-A-v-Q-D-F-V-Q-W-L-M-N-T

THYMOPOIETIN II FRAGMENT 32-36

R-K-v-D-V-Y

Figure 24. Amino acid sequence of glucagon. Protease-3 has nine cleavage sites on glucagon as shown. Eight peptides generated from glucagon were identified by ESIMS (Figure 26). The numbers correspond to the peaks on HPLC chromatography (Figure 25).

PEPTIDE BOND SPECIFICITY OF PROTEASE-3

GLUCAGON

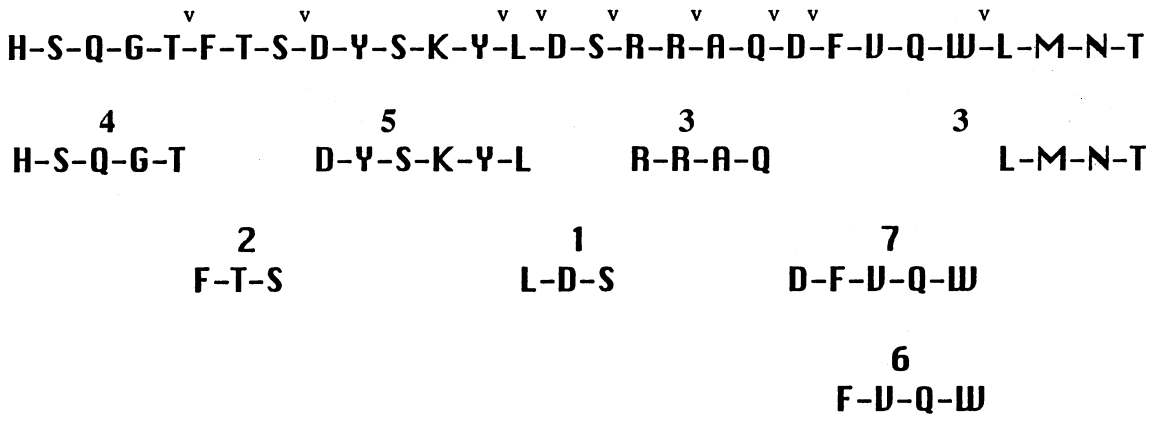

Figure 25. Chromatography on a C_{18}-reverse phase HPLC column of a peptide mixture from *Xcm* protease-3 digestion of glucagon. Peak-1 is A-Q, L-D-S plus R-R, peak-2 is F-T-S, peak-3 is L-M-N-T and R-R-A-Q, peak-4 is H-S-Q-G-T, peak-5 is D-Y-S-K-Y and D-Y-S-K-Y-L, peak-6 is F-V-Q-W, peak-7 is D-F-V-Q-W, peak-8 is uncleaved glucagon. Masses for all peptides listed were identified by Electrospray Mass Spectrometry, and peptide assignments to the numbered peaks are based on ESIMS results for the individual peaks.

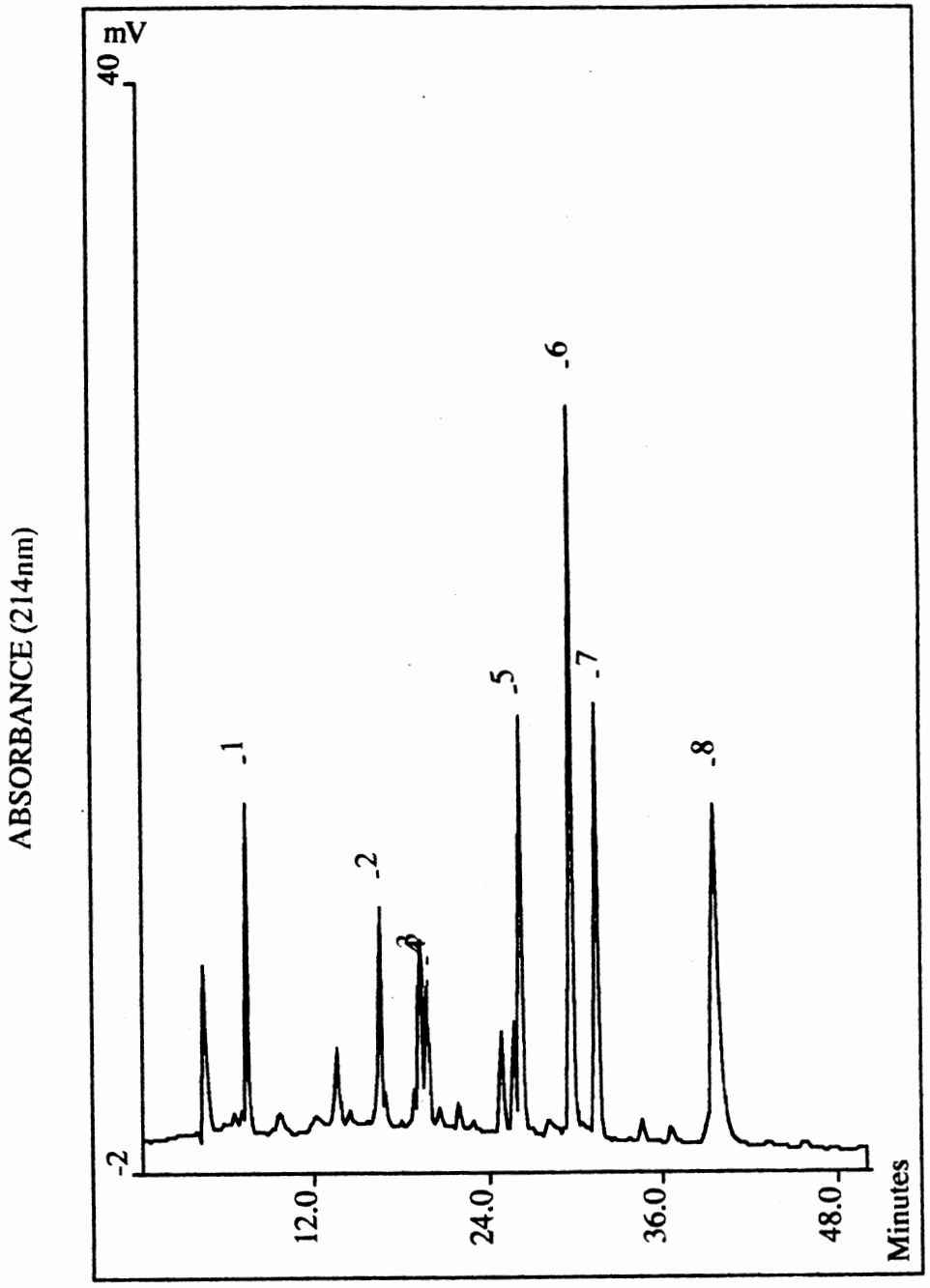
mV
40
-2
.1
.2
.3
.5
.6
.7
.8
12.0
24.0
36.0
48.0
Minutes
ABSORBANCE (214nm)
RETENTION TIME

Figure 26. Electrospray Mass spectrum of peptides obtained by *Xcm* protease-3 cleavage of glucagon. Masses of 257.0 and 301.0 are as predicted for $[M+NH_4^+ + Na^+]$ and $[M+NH_4^+ + 3\ Na^+]$ respectively for the peptide A-Q. Masses of 354.0 and 376.0 are as predicted for $[M+H^+]$ and $[M+Na^+]$ respectively for the peptide F-T-S and also predicted for $[M+Na^+]$ and $[M+2\ Na^+]$respectively for the peptide L-D-S. Masses of 478.0 and 500.0 are as predicted for $[M+H^+]$ and $[M+Na^+]$ respectively for the peptide L-M-N-T. Mass of 529.0 is as predicted for $[M+H^+]$ for the peptides H-S-Q-G-T and R-R-A-Q. Masses of 579.0 and 601.0 are as predicted for $[M+H^+]$ and $[M+Na^+]$ respectively for the peptide F-V-Q-W. Mass of 673.0 is as predicted for $[M+H^+]$ for the peptide D-Y-S-K-Y. Masses of 694.0 and 716.0 are as predicted for $[M+H^+]$ and $[M+Na^+]$ respectively for the peptide D-F-V-Q-W. Masses of 788.5 and 810.0 are as predicted for $[M+H^+]$ and $[M+Na^+]$ respectively for peptide D-Y-S-K-Y-L.

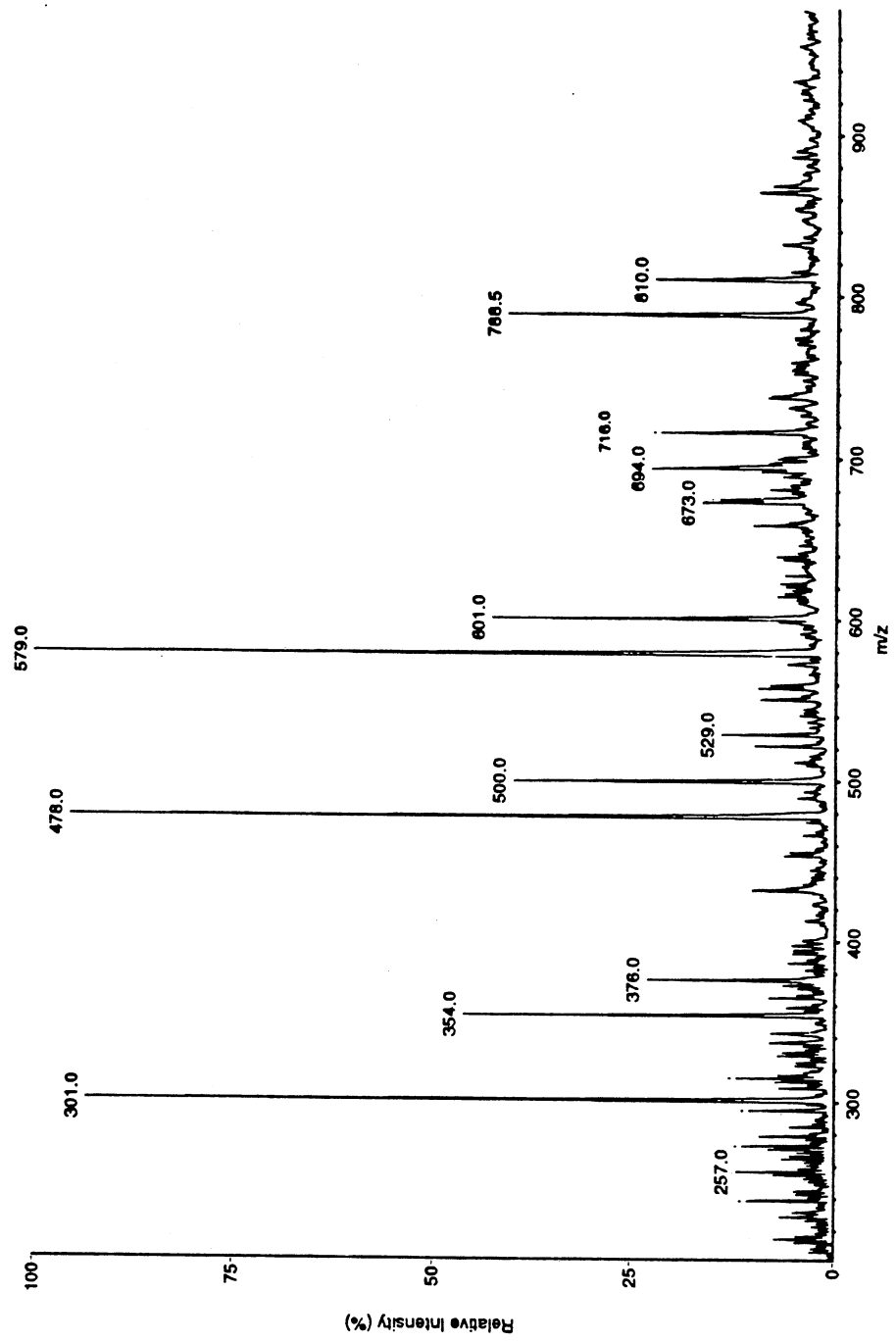
Relative Intensity (%)
100
75
50
25
0
257.0
301.0
354.0
376.0
478.0
500.0
529.0
579.0
601.0
673.0
694.0
716.0
788.5
810.0
300
400
500
600
700
800
900
m/z

Figure 27. Amino acid sequence of oxidized insulin B chain. Protease-3 has ten cleavage sites on insulin B chain as shown. Nine peptides generated from oxidized insulin B chain were identified by ESIMS (Figure 28).

PEPTIDE BOND SPECIFICITY OF PROTEASE-3

OXIDIZED INSULIN B CHAIN

F-V-N-Q-H-L-C(SO_3H)-G-S-H-L-V-E-A-L-Y-L-V-C(SO_3H)-G-E-R-G-F-F-Y-T-P-K-A

7 F-V-N-Q-H

6 C(SO_3H)-G-S-H

2 A-L-Y

5 C(SO_3H)-G-E-R-G

3 L-V-E

1 L-Y

8 L-V-E-A-L-Y

4 L-V-E-A

9 F-F-Y-T-P-K

Figure 28. Electrospray Mass spectrum of peptides obtained by *Xcm* protease-3 cleavage of oxidized insulin B chain. Mass of 295 is as predicted for $[M+H^+]$ for the peptide L-Y. Mass of 364 is as predicted for $[M+H^+]$ for the peptide A-L-Y. Masses of 384 and 408 are as predicted for $[M+Na^+]$ and $[M+2Na^+]$ for the peptide L-V-E. Masses of 431 and 453 are as predicted for $[M+H^+]$ and $[M+Na^+]$ respectively for the peptide L-V-E-A. Mass of 552 is as predicted for $[M+H^+]$ respectively for the peptide of C-G-E-R-G. Masses of 564 and 586 are as predicted for $[M+H^+]$ and $[M+Na^+]$ for the peptide L-C-G-S-H. Masses of 644 and 666 are as predicted for $[M+H^+]$ and $[M+Na^+]$ for the peptide F-V-N-Q-H. Mass of 726 is as predicted for $[M+NH_4^+]$ for peptide L-V-E-A-L-Y. Mass of 803 is as predicted for $[M+H^+]$ for the peptide F-F-Y-T-P-K.

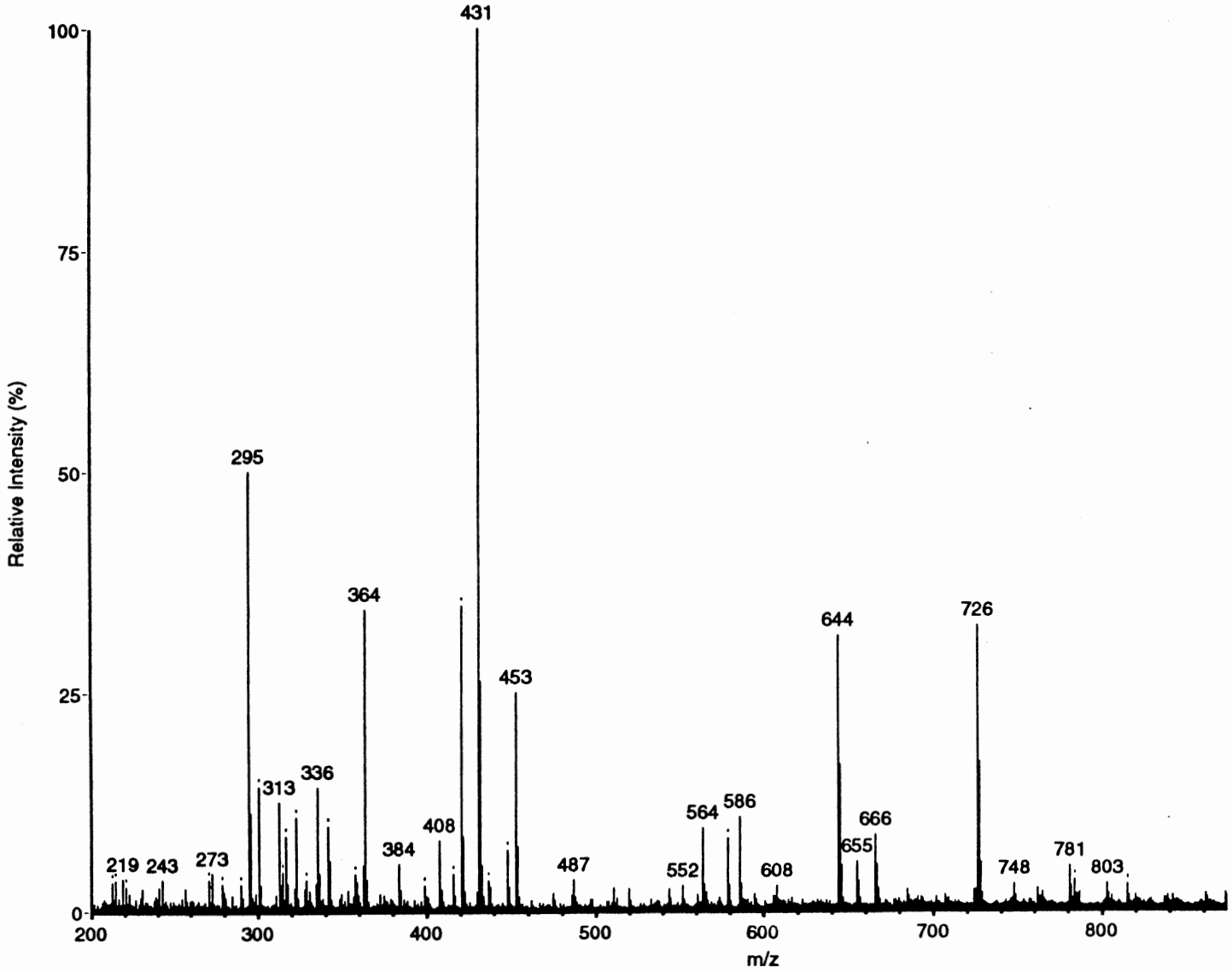
Relative Intensity (%)
100
75
50
25
0
200
300
400
500
600
700
800
m/z
431
295
364
453
644
726
336
313
564
586
666
408
384
655
781
219
243
273
487
552
608
748
803

Figure 29. Amino acid sequence of oxidized insulin A chain. Protease-3 has six cleavage sites on insulin A chain as shown. Five peptides generated from oxidized insulin A chain were identified by ESIMS (Figure 30).

PEPTIDE BOND SPECIFICITY OF PROTEASE-3

OXIDIZED INSULIN A CHAIN

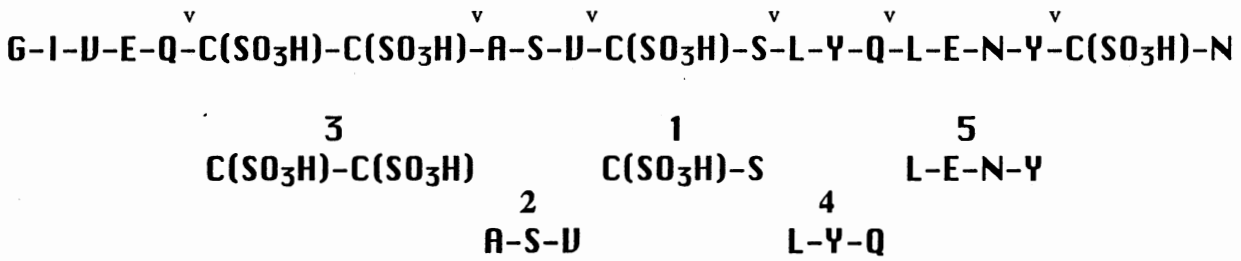

Figure 30. Electrospray Mass spectrum of peptides obtained by *Xcm* protease-3 cleavage of oxidized insulin A chain. Mass of 257 is as predicted for $[M+H^+]$ for the peptide C-S. Masses of 278 and 301 are as predicted for $[M+H^+]$ and $[M+Na^+]$ for the peptide A-S-V. Masses of 359 and 381 are as predicted for $[M+H^+]$ and $[M+Na^+]$ for the peptide C-C. Mass of 462 is as predicted for $[M+2NH_4^+]$ for the peptide L-Y-Q. Mass of 596 is as predicted for $[M+3NH_4^+]$ for the peptide L-E-N-Y.

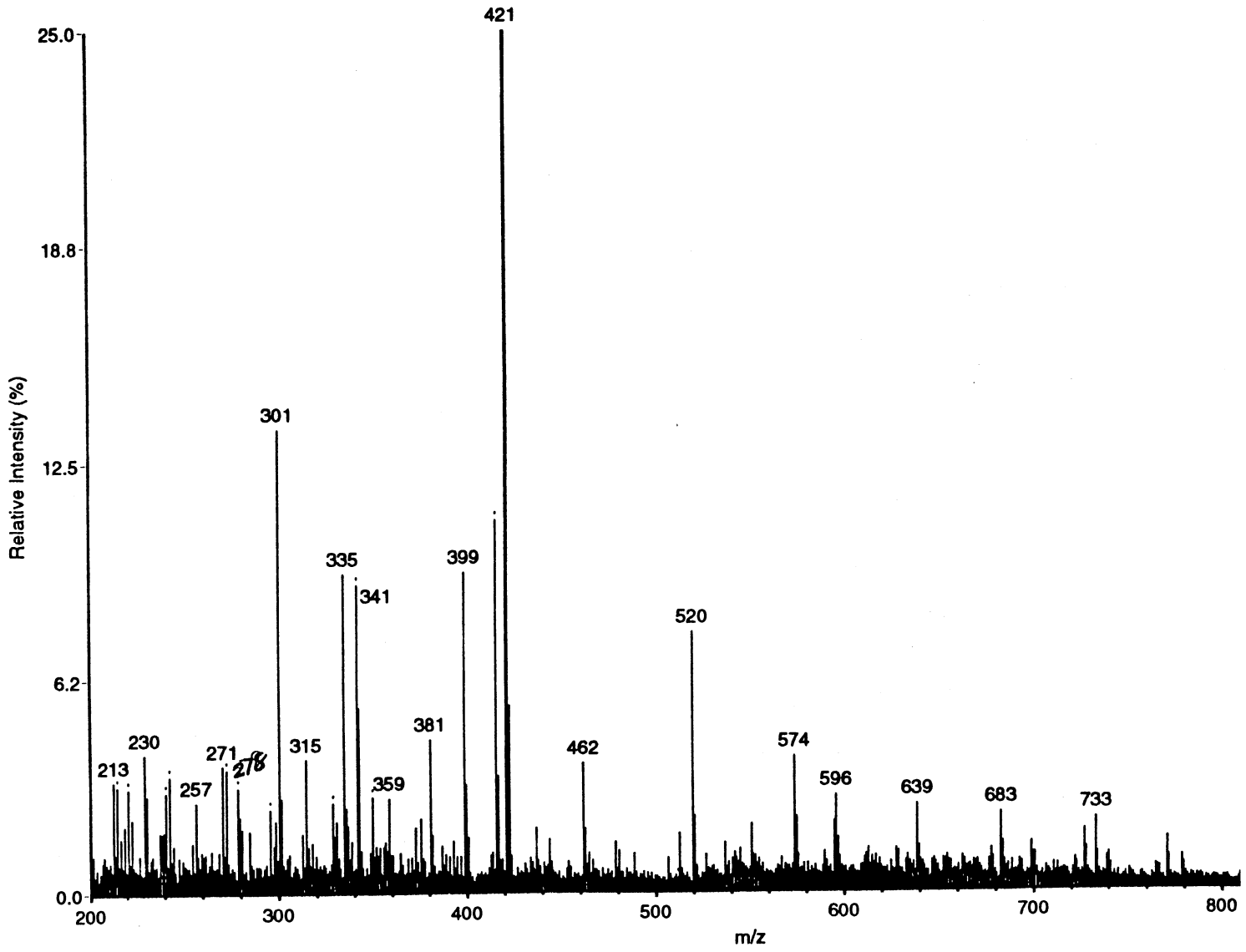
421
25.0
18.8
12.5
6.2
0.0
Relative Intensity (%)
301
335
341
399
520
381
315
230
213
271
257
359
462
574
596
639
683
733
200
300
400
500
600
700
800
m/z

Figure 31. Peptide bond specificity of protease-3 was tested with oxidized insulin B chain, oxidized insulin A chain and glucagon. The purified protease-3 cleaved on the N-terminal side of alanine, leucine, phenylalanine and arginine in addition to cysteic acid on oxidized insulin A and B chains and aspartic acid on glucagon.

PEPTIDE BOND SPECIFICITY OF PROTEASE-3

OXIDIZED INSULIN B CHAIN

F-V-N-Q-H-L-C(SO_3H)-G-S-H-L-V-E-A-L-Y-L-V-C(SO_3H)-G-E-R-G-F-F-Y-T-P-K-A

OXIDIZED INSULIN A CHAIN

G-I-V-E-Q-C(SO_3H)-C(SO_3H)-A-S-V-C(SO_3H)-S-L-Y-Q-L-E-N-Y-C(SO_3H)-N

GLUCAGON

H-S-Q-G-T-F-T-S-D-Y-S-K-Y-L-D-S-R-R-A-Q-D-F-V-Q-W-L-M-N-T

Figure 32. Chromatography on a C_{18}-reverse phase HPLC column of a peptide mixture from oxidized insulin B chain digested by mixture of protease-2 (majority in the mixture) and protease-3 (graph A), and by purified protease-3 (graph B) (4 h incubation at 30° C).

ABSORBANCE (214nm)

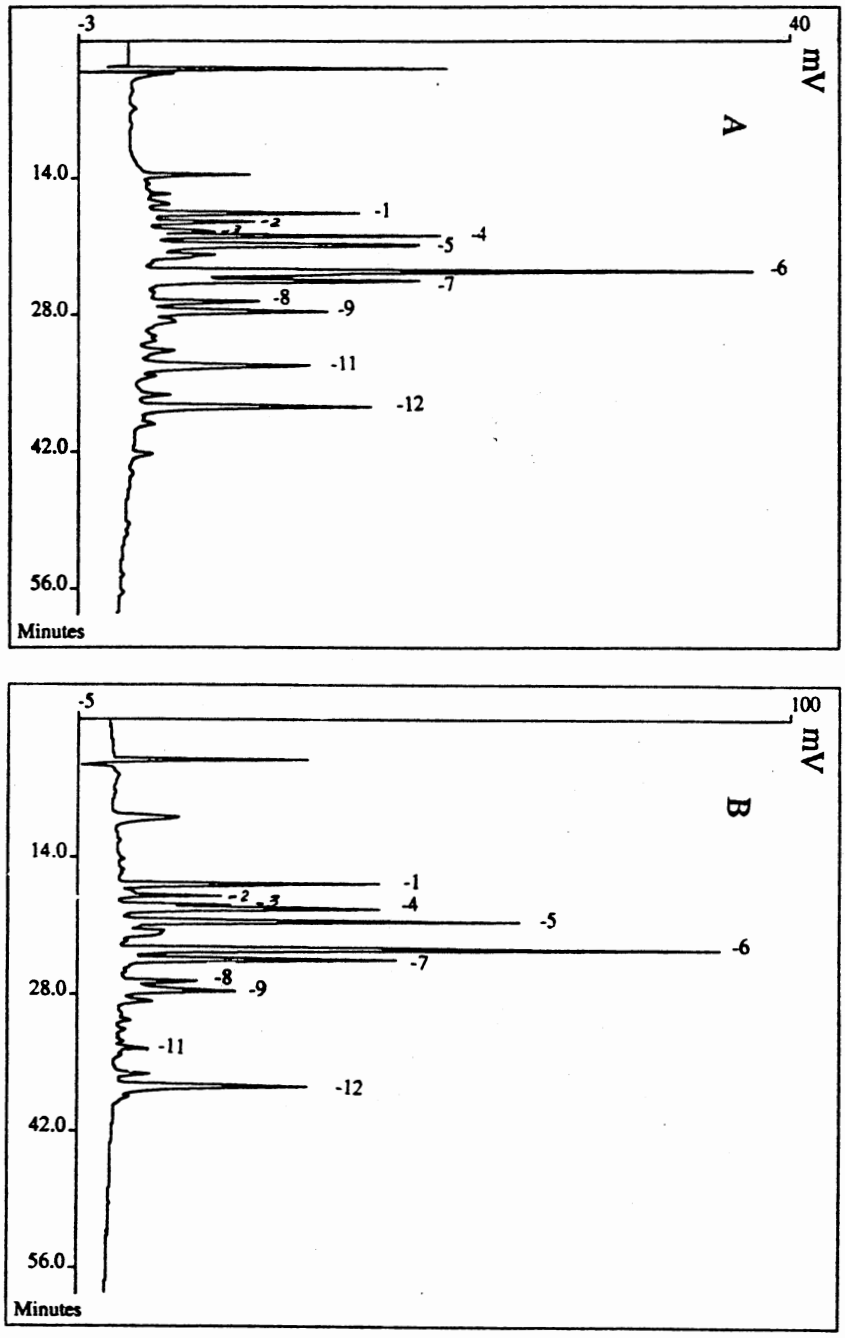

CHAPTER V

SUMMARY AND CONCLUSION

The cotton pathogen *Xanthomonas campestris* pv. *malvacearum* (*Xcm*) produces extracellular proteases which are regulated by nutritional factors. Appreciable protease activity is produced by *Xcm* culture only when protein is present in the growth media (Figure 1). It is possible that the protease inducer is a peptide (s) with N-terminal aspartate which would be formed by a low constitutive level of *Xcm* protease. The requirement for protein in the growth medium for protease secretion by *Xcm* may also be related to the fact that this organism is a pathogen. Protease activity was induced in Xcm when cotton cotyledons were inoculated with the bacteria, and protease activity appeared to contribute to disease development in susceptible cotton plants (Gholson et al., 1987). It is not known whether the proteases characterized here are also the major extracellular proteases expressed by *Xcm in planta.*

To lay groundwork for understanding whether protease produced by *Xcm* are involved in cotton blight pathogenesis, two extracellular proteases, protease-1 and protease-3, were purified from a streptomycin-resistant strain derived from an Oklahoma field isolate of *Xcm* by a combination of procedures. The bacterial culture supernatant containing proteases was first mixed with CM-52 cation exchange resin. The proteases adsorbed on the resin were eluted by a salt gradient, and then purified by DEAE anion exchange chromatography. The mixture of three proteases purified by the above anion exchange chromatography was then subjected to Octyl-sepharose reverse phase chromatography, and protease-1 and protease-3 were thereby purified to apparent homogeneity (only one band was shown in SDS-PAGE). Protease-2 was still present in mixture with a small amount of

protease-3. The molecular weights of protease-1, protease-2 and protease-3 are estimated to be about 29,000, 38,000 and 43,000, respectively by polyacrylamine gel electrophoresis in the presence of sodium dodecyl sulfate.

Protease-1 and protease-3 are active in a broad pH range of 5.5 to 9.5 and both exhibit their maximum proteolytic activity at pH 5.5 to 7.5. Protease-1 and protease-3 are inhibited by EDTA, phosphoramidone and 1,10-phenanthroline, but not by the serine protease inhibitors PMSF and 3,4-Dichloroisocoumarin. This inhibition pattern is very similar to that of the metalloprotease thermolysin. This indicates that protease-1 and protease-3 are metalloproteases rather than serine proteases. In addition, the inhibition of protease-1 activity by EDTA or 1,10-phenanthroline could be reversed by certain metal ions such as Zn^{++} and Mn^{++}. Protease-3 inhibited by EDTA and 1:10-phenanthroline could be reversed by Zn^{++}, Mg^{++} and Mn^{++}. This result suggests that metal ions are required for protease-1 and protease-3 activity, or stability, or both.

The results from this work demonstrate that *Xcm* produces at least three major extracellular proteases (protease-1, protease-2 and protease-3). Purified protease-1 and protease-3 belong to same protease classes, but show different patterns of peptide bond cleavage. The peptide bond specificity of protease-1 was studied using oxidized insulin A chain, oxidized insulin B chain, glucagon, and the Thymopoietin II Fragment 32-36. After treating these substrates with protease-1, the digested peptides were subjected to reverse phase HPLC and identified by either LSIMS or electrospray mass spectrometry. Results obtained from reverse phase HPLC and mass spectrometry revealed that glucagon and thymopoietin II Fragment 32-36 were cleaved on the N-terminal side of aspartic acid residue, and insulin A chain and insulin B chain were cleaved on the N-terminal side of the oxidized cysteine, i.e. cysteic acid (no aspartic acid residue is present in insulin A or B chain). The cleavage at cysteic acid by this protease is due to the similarity between aspartic acid and cysteic acid both in size and in charge. Since cysteic acid is not a normal

constituent of proteins, it is apparent that the natural cleavage site of protease-1 is on the N-terminal side of aspartic acid residues.

The peptide bond specificity of protease-3 was also investigated with glucagon, oxidized insulin A chain and B chain. From HPLC and electrospray mass spectrometry, it was noted that in addition to the N-terminal side of aspartic acid, protease-3 also cleaved glucagon on the N-terminal side of alanine, phenylalanine, leucine and arginine. This is an unusual peptide bond cleavage pattern. The amino acids aspartic acid, alanine, leucine, phenylalanine and arginine have nothing (in size, polarity of side chain or structure) in common. There is a possibility that protease-3 may be a mixture of proteases which are with the same M.W. and charges.

The cleavage peptides produced from oxidized insulin B chain by a mixture (on SDS-PAGE, protease-2 showed a much stronger band than protease-3, which indicated that protease-2 was the majority in the mixture) of protease-2 and protease-3 compared with purified protease-3 appeared (Figure 29) to be identical. This suggests that protease-2 may be derived from protease-3 by protein processing or by proteolytic cleavage during isolation. The mixture of protease-2 and protease-3 has a higher specific activity than purified protease-1 or protease-3 in the azocasein assay.

Of the many proteases which have been characterized, only a very few are as specific as protease-1 in that they cleave peptide bonds adjacent to only one amino acid (see literature review). It appears that the *Xcm* protease-1 is the only protease so far isolated from a wild-type organism which specifically cleaves N-terminal to aspartic acid. Protease-1 with its high peptide bond specificity could be very useful for protein sequence analysis and the production of specific peptides from larger proteins.

REFERENCES

Aebersold, R.H., Leavitt, J., Saavedra, R.A., Hood, L.E., and Kent, S.B.H., Proc. Natl. Acad.Sci. USA , Vol. 84, 6970 (1987).

Al-Mousawi, A.H., Richardson, P.E., Essenberg, M., and Johnson, W.M., Phytopathology , 72, 1222 (1982).

Al-Mousawi, A.H., Richardson, P.E., Essenberg, M., and Johnson, W.M., Phytopathology , 73, 484 (1983).

Ball, A.M., Ashby, A.M., Daniels, M.J., Ingram, D.S., and Johnstone, K., Physiological and Molecular Plant Pathology , 38, 147 (1991).

Barrett, A.J., Introduction: the classification of proteases. Ciba Found. Symp., 75, 1 (1980).

Barrett, A.J., and Salvesen, G., Proteinase Inhibitors. (Amsterdam, New York, Oxford: Elsevier) 16 (1986).

Barry, F.P., Doonan, S., and Ross, C.A., Biochem.J., 193, 737 (1981).

Bashan, Y., Okon, Y., and Henis, Y., Physiological and Molecular Plant Pathology 28, 15 (1986).

Borkar,S. G., and Verma, J.P., Indian Journal of Experiment Biology, Vol. 28, 699 (1990)

Brinkerhoff, L.A., Verhalen, L.M., Johnson, W.M., Essenberg, M., and Richardson, P.E., Plant Disease, 68, 168 (1984).

Cason, E.T., Jr., Richardson, P.E., Brinkerhoff, L.A., and Gholson, R.K., Phytopathology , 67, 195 (1977).

Cason, E.T., Jr., Richardson, P.E., Essenberg, M.K., Brinkerhoff, L.A., Johnson, W.M., and Venere, R.J., Phytopathology , 68, 1015 (1978).

Chowdhury, H.D., Ph.D.Thesis, Indian Agricultural Rasearch Institute, New Delhi, 154 (1978).

Daniels, M.J., Barber, C.E., Turner, P.C., Cleary, W.G., and Sawczyc, M.K., J.Gen. Microbiol., 130, 2447 (1984).

Doonan, S., Doonan, H.J., Hanford, R., Vernon, C.A., Walker, J.M., Bossa, F., Barra, D., Carloni, M., Fasella, P., Riva, F., and Walton, P.L., FEBS Lett., 38, 229 (1974).

Doonan, S., and Fahmy, H.M.S., Eur.J.Biochem., 56, 421 (1975).

Dow, M.J., Clarke, B.R., Milligan, D.E., Tang, J.L., and Daniels, M.J., Applied and Environmental Microbiology, 56, 2994 (1990).

Drapeau, G.R., J. Biol.Chem., 255, 839 (1980).

Drapeau, G. R., Boily, Y., and Houmard, J., J. Biol. Chem., 247, 6720 (1972).

El-Banoby, E.E., and Rudolph, K., Physiol. Plant Pathol., 15, 341 (1979).

El-Banoby, E.E., and Rudolph, K., and Mendgen, K., Physiol. Plant Pathol., 18, 91 (1981)

Essenberg, M., Cason, E.T., Jr., Hamilton, B., Brinkerhoff, L.A., Gholson, R.K., and Richardson, P. E., Physiol. Plant Pathol., 15, 53 (1979a).

Essenberg, M., Doherty, M. d'A., Hamilton, B.K., Henning, V. T., Cover, E. C., McFaul, S.J., and Johnson, W.M., Phutopathology , 72, 1349 (1982).

Essenberg, M., Grover, P.B., and Cover, E.C., Phytochemistry, Vol. 29, No. 10, 3107 (1990).

Essenberg, M.K.,Hamilton, B., Cason, E.T.,Jr., Brinkerhoff, L.A., Gholson, R.K., and Richardson, P.E., Physiol. Piant Pathol., 15, 69 (1979b).

Essenberg, M., and Pierce, M., "Role of Phytoalexins in Resistance of Cotton to Bacterial Blight." in Bacterial Pathogenesis and Disease Resistance. Ed. by D.D. Bills, (1992 in press).

Essenberg, M., Pierce, M., Shevell, J.L., Sun, T.J., and Richardson, P.E., Sesquiterpenoid phytoalecxins and resistance of cotton to *Xanthomonas campestris* pv. *malvacearum.* In Current Communications in Molecular Biology: Plant Cell / Cell Interactions, Sussex, I., Ellingboe, A., Crouch, M., and Malmbreg, R., eds., Cold Spring Harbor Laboratory, New York. 145 (1986).

Fenn, J.B., Mann, M., Meng, C.K., and Wong, S.F., Mass Spectrometry Reviews. Vol. 9, 37 (1990)

Gholson, R.K., and Essenberg, M., Federation Proceedings Vol. 46, 2212 (1987).

Gholson, R.K., Rodgers, C., and Pierce, M., Phytopathology 79, 1199 (1989),

Gholson, R.K., Rodgers, C., Mitchell, E.D.,and Rogers, J.B., FASEB J. 4 A2159 (1990)

Gholson, R.K., Rodgers, C., and Essenberg, M., FASEB J.2 A1115 (1988)

Heinrikson, R.L., and Meredith, S.C., Anal. Biochem., 136, 65 (1984).

Hinode, D., Hayashi, H., and Nakamura, R., Infection and Immunity, 3060 (1991)

Ingrosso, D., Fowler, A.V., Bleibaum, J., and Clarke, S., Biochem. Biophys. Res. Commun., 162, 1528 (1989).

Jensen, S.E., Phillippe, L., Teng Tseng, J., Stemke, G.W., and Campbell, J.N., Can. J.Microbiol., 26, 77 (1980).

Keesey, J. Biochimica information. Boehringer Mannheim., (1987).

Kyostio, S.R.M., Cramer, C., and Lacy, G.H., J. of Bacteriology, 6537 (1991).

Levy, M., Fishman, L., and Schenkein, I., Methods in Enzymol., 19, 672 (1970).

Liu, Y.N., Tang,J.L., Clarke, B.R., Dow, J.M., and Daniels, M,J., Mol. Gen. Genet 220, 433 (1990).

Lushbaugh, W.B., Kairalla, A.B., Hofbauer, A.F., Arnaud, P., Cantey, J.R., and Pittman, F.E., Am.J.Trop.Med.Hyg., 30, 575 (1981)

McNally, K., Gabriel, D., and Essenberg, M., Phytopathology , 74, 875 (1984).

Morgham, A.T., Richardson, P.E., Essenberg, M., and Cover, E.C., Physiol. Mol. Plant Pathol., 32, 141 (1988).

Neidhardt, F.C., Bloch, P.C., and Smith, D.F., J. Bacteriol., 119, 736 (1974).

Niven, G.W., J. General Microbiology , 137, 1207 (1991).

Noreau, J., and Drapeau, G.R., J.Bacteriol., 140, 911 (1979).

North, M.J., Microbiol. Rev., 46, 308 (1982).

Ogrydziak, D.M., and Scharf, S.J., Journal of General Microbiology , 128, 1225 (1982).

Ries, S.M., and Alberheim, P., Phytopathology , 63, 625 (1973).

Roby,D., Toppan,A., and Esquerre-Tugaye, M., physiological and molecular Plant Pathology 30, 453 (1987).

Royer, G.P., Hsiao, H.Y., and Anantharamaiah, G.M., Biochimie, 62, 537 (1980).

Samsinakova, A., Bajari, C., Kalalova, S., Kmitowa, K., and Wocziechowska, M., Bull. Acad. Pol. Sci. Ser.Sci.Biol., 25, 521 (1977).

Seferiadis, K., Frillingos, S., and Tsolas, O., Chromatogram, 2 (1987).

Shipolini, R.A., Callewaert, G.L., Cottrell, R.C., and Vernon. C.A., Eur. J. Biochem., 43, 465 (1974).

Smith, P.K., Krohn, R.I., Hermanson, G.T., Mallia, A.K., Gartner, F.H., Provenzano, M.D., Fujimoto, E.K.,Goeke, M.N., Olson, B.J., and Klenk, D.C., Analytical Biochemistry , 150, 76 (1985).

Smith, R.D., Loo, J.A., Ogorzalet Loo, R.R.,Buaman, M., and Udseth, H.R., Mass spectrometry reviews. Vol.10, No. 5, 359 (1991).

Starr, M.P., The Genus *Xanthomonas,* Chapter 62, in [Starr, M.P., Stolp, H., Triiper, M.G., Balows, A., and Schlegel, H.G., eds.] (The Prokaryotes) Brelin: Springer-Verlag., 742 (1981).

Steidl, J. R., (Ph.D. dissertation, Oklahoma State University) 150 (1988).

Sun, T.J., (Ph.D. dissertation, Oklahoma State University) 145 (1987).

Sun, T.J., Melcher, U., and Essenberg, M., Physiol. Mol. Plant Pathol., 33, 115 (1988).

Thakur, R.P., Kumar, S., Patel, P.N., and Verma, J.P., Indian Phytopathol., 31, 52 (1978).

Verma, J.P., Bacterial Blight of Cotton. (Boca Raton, FL: CRC Press, Inc.) 93 (1986).

Verma, J.P., and Singh, R.P., Indian Phytopathol., 28, 379 (1975)

Walton, P.L., Turner, R.W., and Broadbent, D., U.K. Pat. No.1263956; Walton, P.L., Jones, C., and Jackson, S., to be published. (1972).

Weber, K., Pringle, J. R., and Osbirne, M., Methods in Enzymol., 26, 3 (1972).

Widmer, F., and Johansen, J.T., Carlsberg Res.Commun., 44, 37 (1979).

Wolf, D.H., Proteinases and sporulation in yeast. Academic Press Inc., London. 355 (1981).

Wood, P. J., and Siddiqui, I. R., Carbohydr. Res., 22, 212 (1972).

VITA 2

Jing Huang

Candidate for the Degree of

Master of Science

Thesis: PURIFICATION AND CHARACTERIZATION OF TWO EXTRACELLULAR PROTEASES WITH UNUSUAL PEPTIDE BOND SPECIFICITY FROM *XANTHOMONAS CAMPESTRIS* PV.*MALVACEARUM*

Major Field: Biochemistry

Biographical:

Personal Data: Born in Shenyang, China, March 15, 1956, the daughter of Jianren Huang and Shuyun Gao.

Education: Graduated from Shongling High School, Shenyang, China, in July 1974; received Bachelor of Science Degree in Animal Science from Shenyang Agricultural University, Shenyang, China, in July, 1982; completed requirements for the Master of Science Degree at Oklahoma State University in May, 1992.

Professional Experience: Research Assistant in Biochemistry, Oklahoma State University, Stillwater, Oklahoma June, 1990, to May, 1992; Teaching Assistant in Biochemistry, Oklahoma State University, Stillwater, Oklahoma January, to May, 1991 and January, to May, 1992.